

**Compositional Analysis of the Lokoja Formation, Bida  
Basin and Its Implication on the Provenance and  
Paleoenvironments.**

**by**

**Oluwakotanmi Timothy Taiwo**

**GLY/14/2259**

**Submitted**

**to the**

**Department of Geology.**

**in**

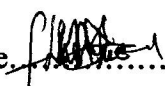
**Partial Fulfilment of the Requirements for the Award  
of Bachelor of Science (B.Sc.) Degree in Geology**

**February, 2019**

**CERTIFICATION**

This is to certify that the research project on the Compositional Analysis of the Lokoja Formation, Bida Basin and It's Implication on the Provenance and Paleoenvironments was actually carried out by Oluwakotanmi Timothy Taiwo with matriculation number GLY/14/2259 under the supervision of Prof. O.J Ojo.

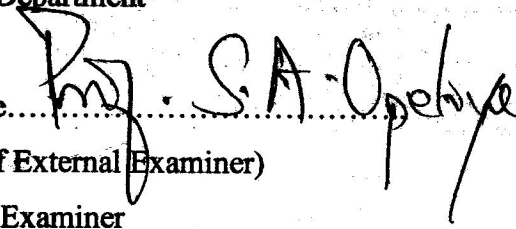
The work has been approved as meeting the required standard for the award of Bachelor of Science (B.Sc.) Degree of the department of Geology, Faculty of Science, Federal University Oye-Ekiti, Ekiti State, Nigeria.

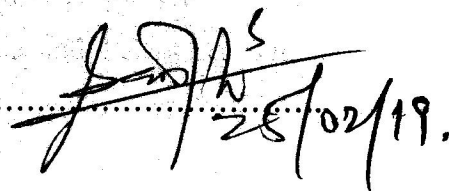
Signature  .....  
Project Supervisor

Date 19/02/2019

Signature .....  
Prof. O.J. Ojo  
Head of Department

Date.....

Signature  .....  
(Name of External Examiner)  
External Examiner

Date  28/02/19.

## **DEDICATION**

I dedicate this Project work to the Almighty God for the grace and strength He accorded me, and to my parents, Pastor Dr. & Dns I.G Awotanmi, for their support morally and financially.

## ACKNOWLEDGEMENTS

I would like to appreciate God Almighty for His grace and strength He bestowed on me during the course of this project work. My profound gratitude goes to my Supervisor, Professor O.J Ojo for his immense contribution towards the success of this Project. I appreciate my parents, Pastor Dr. & Dns I.G Awotanmi, for their support financially and morally, also to my lecturers: Mr T.A Bolaji, Mrs N.O Okon, Mr M.O Adeoye, Mr E.C Chukwu, and Miss J. Oyebamiji, you are all appreciated. To my colleges: Precious, Emmanuel, Barakat, Rachel, Tosin, Samuel, Razaq and co. you are all appreciated.

## Table of Contents

Title page	i
Certification/approved page	ii
Dedication	iii
Acknowledgement	iv
Table of contents	v
List of Figures	vii
List of Tables	ix
List of Plates	x
Abstract	xi
<b>CHAPTER ONE: INTRODUCTION</b>	
1.1 Background Information	1
1.2 The Area of Study (Location, Extent and Accessibility)	3
1.3 Physiography	5
1.4 Climate	5
1.5 Vegetation	6
1.6 Occupation of the inhabitants of the Study Area.	6
1.7 Previous work	6
1.8 Aim and Objectives of the study	7
<b>CHAPTER TWO: REGIONAL GEOLOGY</b>	
2.1 Tectonic setting of the Bida Basin	8
2.2 Stratigraphy of the Bida Basin	8
<b>CHAPTER THREE: MATERIALS AND METHODS</b>	
3.1.1 Materials	11
3.1.2. Methods	12
3.2.1 Field mapping and Sample Collection	12
3.2.2 Processing and analyses of the Samples	13
3.2.3 Pebble Morphometry	13

3.2.4	Techniques for preparation of thin section	14
3.2.5	Granulometric Analysis	14
3.2.6	Geochemistry	16
<b>CHAPTER FOUR: RESULTS AND DISCUSSIONS</b>		
4.1	Lithostratigraphy	17
4.2	Texture	27
4.2.1	Pebble Morphometry	27
4.2.2	Grain size data	35
4.3	Petrography	46
4.4	Heavy Mineral Analysis	51
4.5	Geochemistry	55
4.6	Provenance	58
4.7	Paleoenvironments	61
<b>CHAPTER FIVE: CONCLUSIONS</b>		
5.1	Conclusions	62
	References	63

## List of Figures

<b>Figure</b>	<b>Page</b>
Fig. 1.1: Geological map of Nigeria and location of the study area	2
Fig. 1.2: Geological Map of Study Area Showing Locations of Studied Sections.	4
Fig. 2.1: Stratigraphy of Bida Basin	10
Fig. 4.1: The Lokoja Formation exposed at Filele 1.	18
Fig. 4.2: The Lokoja Formation exposed at Filele 2.	19
Fig. 4.3: The Lokoja Formation exposed at Filele 3.	20
Fig. 4.4: Litholog of Filele 1 outcrop.	21
Fig. 4.5: Litholog of Filele 2 outcrop.	22
Fig. 4.6: Litholog of Filele 3 outcrop.	23
Fig. 4.7: Scattered Plots of the Pebble Forms for FE1B: (a) Plot of sphericity against OP Index showing separation of beach field from the fluvial field; (b) Plot of roundness against elongation ratio; (c) Bivariate plot of Flatness Index and Sphericity Index.	29
Fig. 4.8: Scattered Plots of the Pebble Forms for FE1E: (a) Plot of sphericity against OP Index showing separation of beach field from the fluvial field; (b) Plot of roundness against elongation ratio; (c) Bivariate plot of Flatness Index and Sphericity Index.	30
Fig. 4.9: Scattered Plots of the Pebble Forms for FE2C: (a) Plot of sphericity against OP Index showing separation of beach field from the fluvial field; (b) Plot of roundness against elongation ratio; (c) Bivariate plot of Flatness Index and Sphericity Index.	31
Fig. 4.10: Particle size distribution curve for sample FE1B	33
Fig. 4.11: Particle size distribution curve for sample FE1D	34
Fig. 4.12: Particle size distribution curve for sample FE1E	34
Fig. 4.13: Particle size distribution curve for sample FE2A	35

<b>Fig. 4.14: Particle size distribution curve for sample FE2B</b>	35
<b>Fig. 4.15: Particle size distribution curve for sample FE2C</b>	36
<b>Fig. 4.16: Particle size distribution curve for sample FE3A</b>	36
<b>Fig. 4.17: Particle size distribution curve for sample FE3B</b>	37
<b>Fig. 4.18: Particle size distribution curve for sample FE3C</b>	37
<b>Fig. 4.19: Particle size distribution curve for sample FE3E</b>	38
<b>Fig. 4.20: Particle size distribution curve for sample FE3F</b>	38
<b>Fig. 4.21: Particle size distribution curve for sample FE3G</b>	39
<b>Fig. 4.22: Plots of Mean against Standard deviation.</b>	42
<b>Fig. 4.23: Skewness vs Standard Deviation plots.</b>	42
<b>Fig. 4.24: QFL Ternary Plot of Sandstone in the Study Area.</b>	47
<b>Fig. 4.25: Cross Plots of Major Oxides: SiO<sub>2</sub> against Fe<sub>2</sub>O<sub>3</sub>, SiO<sub>2</sub> against Al<sub>2</sub>O<sub>3</sub>, SiO<sub>2</sub> against L.O.I, Fe<sub>2</sub>O<sub>3</sub> against Al<sub>2</sub>O<sub>3</sub>.</b>	54
<b>Fig. 4.26: Discriminant Function diagram for provenance</b>	56



### List of Table

Table 4.1: Computed and Estimated Morphometric Properties Used in the study	25
Table 4.2: Morphometric Data of Lokoja Formation Pebbles from Filele (FE1E)	25
Table 4.3: Morphometric Data of Lokoja Formation Pebbles from Filele (FE2C)	26
Table 4.4: Morphometric Data of Lokoja Formation Pebbles from Filele (FE1B)	27
Table 4.5: Pebble Morphological Analysis Interpretation	28
Table 4.6: showing the formulas needed for determining the values for interpreting the data acquired.	32
Table 4.7: Grain Size Analysis data for Filele Sandstone.	33
Table 4.8: Percentile values from Cumulative Curve Plots of Sandstone Samples in the Study Area	40
Table 4.9: Table showing Data Interpreted from Calculated Values	41
Table 4.10: Modal Analysis of Sandstone Obtained from Petrography.	46
Table 4.11: Maturity scale of Sandstone.	46
Table 4.12: Percentage Composition of the Non-opaque and Opaque Heavy Mineral Suites in the Study Area	51
Table 4.13: Table showing Major oxides and their percentage.	53

## List of Plates

Plate 3.1: Compass	11
Plate 3.2: A GPS	11
Plate 3.3: A Geological Hammer	11
Plate 3.4: Chisel	11
Plate 4.1: Photomicrograph of Lokoja sandstone FE1B under PPL	44
Plate 4.2: Photomicrograph of Lokoja sandstone FE1B under XPL	44
Plate 4.3: Photomicrograph of Lokoja sandstone FE2A under PPL	44
Plate 4.4: Photomicrograph of Lokoja sandstone FE2A under XPL	44
Plate 4.5: Photomicrograph of Lokoja sandstone FE2D under PPL	45
Plate 4.6: Photomicrograph of Lokoja sandstone FE2A under XPL	45
Plate 4.7: Photomicrograph of Lokoja sandstone FE1A under PPL	45
Plate 4.8: Photomicrograph of Lokoja sandstone FE1A under XPL	45
Plate 4.9: Photomicrograph of heavy minerals in Lokoja sandstone (FE1B)	49
Plate 4.10: Photomicrograph of heavy minerals in Lokoja sandstone (FE1B)	49
Plate 4.11: Photomicrograph of heavy minerals in Lokoja sandstone(FE1C)	49
Plate 4.12: Photomicrograph of heavy minerals in Lokoja sandstone (FE1C)	49
Plate 4.13: Photomicrograph of heavy minerals in Lokoja sandstone(FE2B)	50
Plate 4.14: Photomicrograph of heavy minerals in Lokoja sandstone(FE2B)	50
Plate 4.15: Photomicrograph of heavy minerals in Lokoja sandstone(FE3C)	50
Plate 4.16: Photomicrograph of heavy minerals in Lokoja sandstone(FE3C)	50

### Abstract

Pebble Morphometry, Grain size, Petrography, Heavy mineral analysis and Geochemical analysis were carried out to interpret the paleodepositional environment of the conglomeratic sandstone of the Lokoja Formation. The Lokoja Formation is well exposed along Filele, which is at the outskirts of Lokoja, in the Southern Bida Basin of Nigeria. Pebbles were collected along Okene Abuja highway, the three axes the Long (L), Intermediate (I), and the short (S) were measured for three set(s) of quartzite pebbles, at the first, second and third location 60, 70 and 18 pebbles were picked randomly.

The Results obtained indicate predominance of fluvial processes, with Flatness Ratio (FR) =  $0.61 \pm 0.12$ , Elongation Ratio (ER) =  $0.69 \pm 0.12$ , Maximum Projection Sphericity Index (M.P.S.I) of  $0.81 \pm 0.06$  (Fluviatile) and Oblate Prolate Index of  $1.62 \pm 0.65$ . Roundness was estimated using Same's visual image sets. The mean of these indices confirm a fluvial origin for the pebbles. Plots of Sphericity Index Against Oblate Prolate Index and plots of Coefficient of Flatness against Sphericity Index all indicate or point out to Fluviatile origin of sedimentation. In Addition, plots of roundness versus elongation for the pebbles shows 18% of the pebbles in the littoral field, 32% in the transitional field and 35% in the fluviatile field.

Depositional environments defined by values of binary plots of skewness versus standard deviation mean versus standard deviation for samples obtained from the Lokoja area, indicate that sediments of the Lokoja Formation was deposited in a continental fluvial paleodepositional environment.

The geochemical data shows that Positive correlations with  $Al_2O_3$  are shown by most of the major elements. It can be concluded, therefore, that the enrichment of other major elements in the Lokoja Sediments is related to the enrichment of ferromagnesian minerals and feldspars probably due to short transportation of the source materials. From our heavy mineral analysis we know that the results indicated the dominance of ultra-stable heavy minerals over the metastable and unstable varieties. From the petrographic data studied, the Lokoja sandstone is mineralogically immature and its provenance is not far from the basin in which it was deposited. The results gotten from the grain size analysis agrees with the results gotten from the Pebble Morphometric Analysis.

## CHAPTER ONE

### INTRODUCTION

#### 1.1 Background Information

The Bida Basin (also known as Nupe Basin), is an oval shaped structural intracratonic sedimentary feature, elongated along northwest-southeast direction and perpendicular to the main axis of the Benue Trough (Fig. 1.1). The Bida basin is an area of local subsidence formed during the Campanian–Maastrichtian age, during which the South Atlantic–Tethys seaway was probably routed through the Basin (Ojo and Ajakaiye, 1976). Stratigraphic framework in this basin has been along the geographic subdivision of the basin into north and south Bida basins. In the southern Bida basin, the main stratigraphic units are Campanian – Maastrichtian Lokoja Formation (conglomerate, sandstone), Maastrichtian Patti Formation (sandstone, shale, claystone), and Agbaja Formation (ironstone).

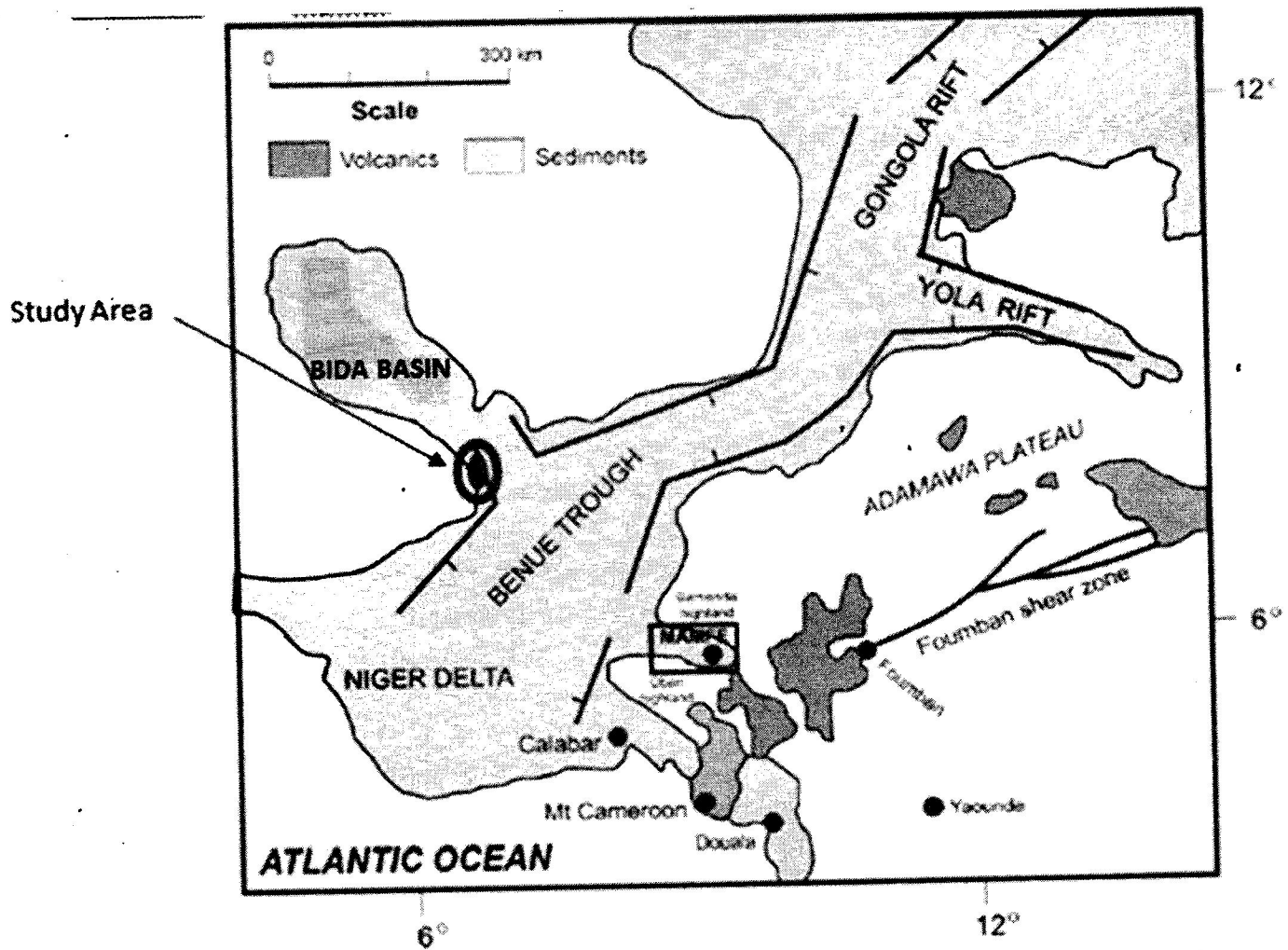
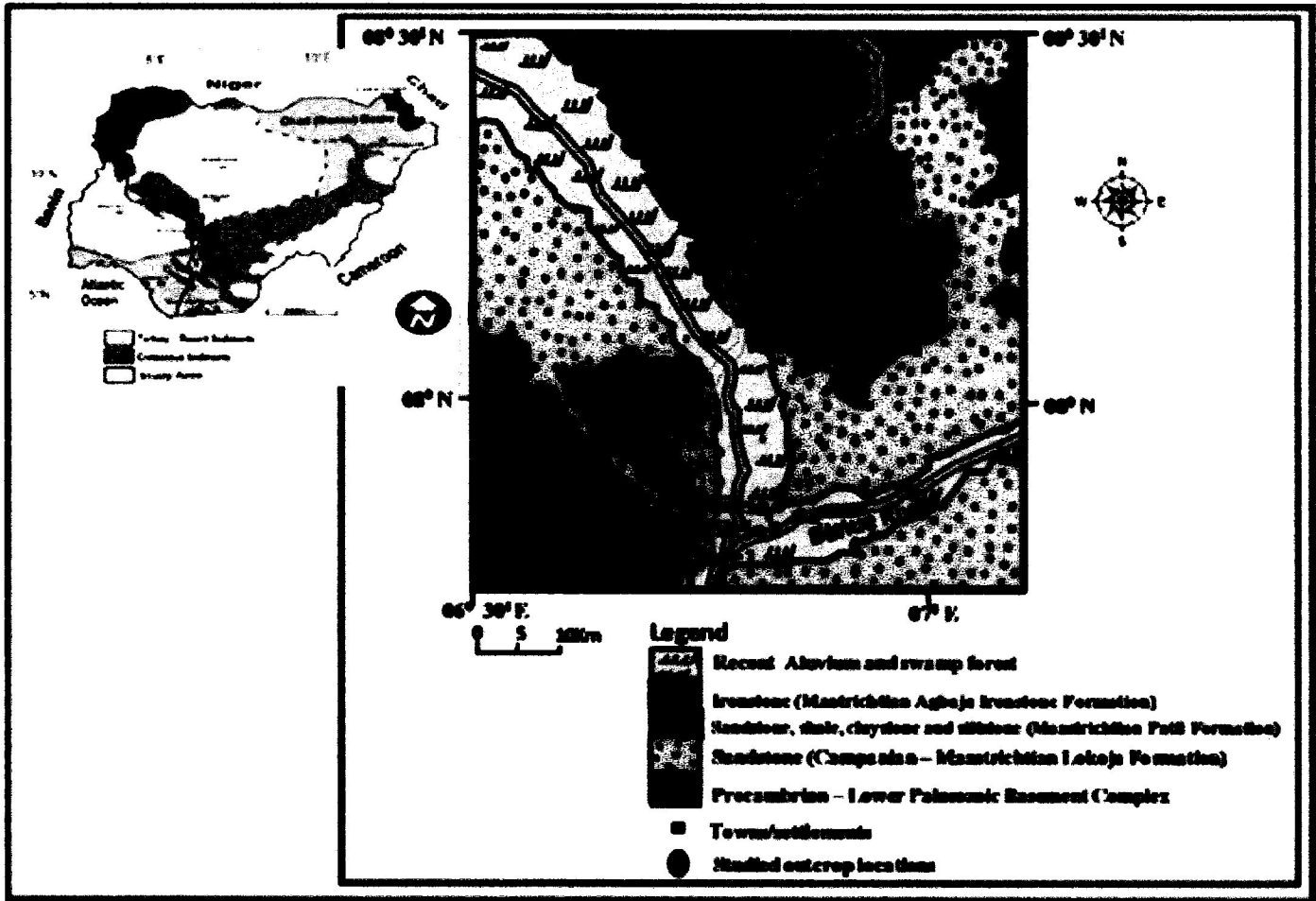


Fig. 1.1: Geological map of Nigeria and location of the study area (Modified from Akande et. al, 2005).

## 1.2 The Area of Study (Location, Extent and Accessibility)

The Bida Basin constitutes a series of Cretaceous and later rift basins in Central and West Africa whose origin is related to the opening of the South Atlantic. The study area covers road cut exposures along the Lokoja – Abuja highway (Fig. 1.2) and lies within latitudes  $07^{\circ} 51'$  to  $08^{\circ} 26'$  and longitudes  $006^{\circ} 41'$  to  $006^{\circ} 56'$ . Samples were taken from three different outcrops located at the outskirts of Lokoja town and lies within Long.  $07^{\circ} 51' 18''$  E, Lat.  $006^{\circ} 41' 54.5''$  N, Long.  $06^{\circ} 042' 43''$ , Lat.  $07^{\circ} 51' 15.0''$  and Lat.  $07^{\circ} 51' 11''$  N, Long.  $06^{\circ} 42' 59''$  E.



**Fig. 1.2:** Geological Map of Study Area Showing Locations, File 1, 2, 3, of Studied Sections with Inset Map of Nigeria Showing NW/SE Trending Bida Basin (Modified After Agyingi, 1991)

### 1.3 Physiography

The dominant physical features of the study area in the western axis are largely mountains coupled with a number of intermittent valleys and rivers crossing the breadth of the subject area. Mount Patti which is the highest point has a height of about 458 meters above sea level and gently reduces in height till it reaches river Niger at the height of 45 meters above sea level. On the other hand, the territory on the East of river Niger is relatively flat but perforated by the presence of low leveled rocks and tributary rivers to rivers Niger and Benue.

### 1.4 Climate

The site has a tropical climate that comprises of two season namely dry and wet seasons. The wet seasons starts from the month of April and ends in October, while the dry season starts from November and continues till March. The two seasons are affected by the south-westerly winds coming from the Atlantic Ocean and north-easterly winds which come from the Sahara Desert. Another weather phenomenon (micro climate) is associated with the presence of inselbergs. This feature exerts an influence on local weather greater than their size.

**Wind Dust:** Two major air masses dominate the climate of the study area. These are the Tropical Maritime air mass and the Tropical continental air mass. The Tropical Maritime is formed over the Atlantic Ocean to the South of the country and is therefore warm and moist. It moves inland generally in a South-West to North-East direction. The Tropical Continental air mass is developed over the Sahara Desert and is therefore warm and dry and blows in the opposite direction, (north-east to south-west). The oscillation between these two air masses produces high seasonal characteristics of weather conditions in the country. The Tropical Continental air mass is associated with the dry season and the Tropical Maritime air mass creates wet season.

**Rainfalls:** There are two seasons, dry and wet; the dry season lasts between October and April in each year while the wet season lasts between May and September. The annual average rainfall ranges between 1000 mm and 1500 mm while the mean annual humidity is about 70%.

**Humidity and Temperature:** The highest temperatures in the study area always tend to occur at the end of the dry season close to the spring equinox. Thus March has the highest temperature of about 34.5°C , while the lowest temperature occur in the middle of the dry season in December/January, when outgoing radiation is encouraged by low humidity, clear skies and longer nights. The temperature at this time falls as low as 22.8°C.



In the dry season there is a decrease in relative humidity from south to north in the study area caused by the higher elevation in the north. In the rainy season, this variation disappears and associated with the high relative humidity is an extensive cloud cover over the region.

### **1.5 Vegetation**

The vegetation of the study area falls within the Guinea Savanna belt of Nigeria. This vegetation type has many variants, affecting both the floristic diversity and the structural appearance of the plant communities. Equally, there are several Forest Reserves in the study area and some of the notable economic trees that can be found in the reserves include Iroko, Mahogany and Obeche. Human activities have however altered drastically the natural vegetation especially in the central zone where urbanization and mining activities predominate. Since Lokoja became an administrative headquarters of Kogi state in 1991, it has been experiencing an explosive population increase which had also led to expansion with significant changes in its physical landscape-land use cover types over the years. The built-up area, vacant land, cultivated land and other land use types increased in the study area at the expense of vegetation cover. For example in 1987, the vegetal cover was about 42.21km<sup>2</sup> and by 2005, it had reduced to 8.41km<sup>2</sup>.

### **1.6 Occupation of the inhabitants of the Study Area.**

It is a trade center with respect to its agricultural products; this is because it is situated at the confluence of the Niger and Benue rivers, and is close to the new federal capital of Nigeria in Abuja. The major occupation of the inhabitants of this area is fishing.

### **1.7 Previous work**

Previous geological investigations in the Bida basin include among others; Falconer (1911), Jones (1953, 1958), Adeleye (1973, 1974, 1989), Jan du Chene *et al.* (1978), Agyingi (1991), Braide (1992), Ladipo *et al.* (1994), Abimbola (1997), Abimbola *et al.* (1999), Ojo and Akande (2003, 2006, 2009), Obaje *et al.* (2004, 2011), Akande *et al.* (2005), Okunlola and Idowu (2012) and Nton and Okunade (2013). These studies covered the geology, stratigraphy, sedimentology, mineralogy and hydrocarbon potential of the different formations within the basin.

Ojo and Akande (2003) and Ojo and Akande (2009) reported on facies relationship and depositional environments of the Upper Cretaceous Lokoja Formation as well as the sedimentology and depositional environment of the Patti Formation within the Bida basin respectively.

## **1.8 Aim and Objectives of the Study**

The aim of the study is to improve on the existing knowledge of the study area by carrying out detailed geological investigation to determine paleoenvironment of deposition and the succession in the area. The following are the objectives of the study:

- i. To decipher the facie and facies association in the study areas.
- ii. To decipher the paleoenvironment of deposition of the sediments in the study areas.
- iii. To evaluate the mineralogical composition or the lithologic units setting in which the sediments were formed.
- iv. To provide the source (provenance) and maturity of the sediments.
- v. To provide the mineralogical and elemental composition of sediments in the area.

## CHAPTER TWO

### REGIONAL GEOLOGY

#### 2.1 Tectonic settings of the Bida Basin

The Bida Basin constitutes a series of Cretaceous and later rift basins in Central and West Africa whose origin is related to the opening of the South Atlantic (Fig. 1.1). The Bida Basin is divided into northern and southern Bida Basin, each varying in lithostratigraphic succession (Adeleye, 1972). The Southern Bida Basin, which is the focus of this study, extends from the confluence of the Niger-Benue River at Lokoja to Abaji, near the Federal capital Territory. It is made up of three formations from oldest to youngest; Lokoja, Patti and Agbaja Formations. The Lokoja Formation is the oldest stratigraphic sequence in the Southern Bida Basin and unconformably overlies the Precambrian Basement Complex. It consists of basal conglomerate, subrounded to well rounded quartz, feldspar, pebbles and cobbles, especially at the sediment–basement contact. The pebbles are embedded in whitish clayey matrix. The basal conglomerate is overlain by fine to very coarsegrained conglomeritic sandstone, coarse-grained, cross bedded sandstone, and few thin oolitic iron stones. The sandstones are continental deposits, generally poorly sorted, composed mainly of quartz and feldspar and therefore texturally and mineralogically immature (Ojo and Akande, 2003).

#### 2.2 Stratigraphy of the Bida Basin

The stratigraphic succession of the Mid-Niger Basin, collectively referred to as the Nupe Group (Adeleye, 1972) comprises a two fold Northern Bida Basin (Sub- Basin) and Southern Bida Sub-Basin or Lokoja Sub-Basin (Fig. 2.1). The Bida Basin is assumed to be a northwesterly extension of the Anambra Basin (Akande et al., 2005). The basin fill comprises a north west trending belt of Upper Cretaceous sedimentary rocks that were deposited as a result of block faulting, basement fragmentation, subsidence, rifting and drifting consequent to the Cretaceous opening of the

South Atlantic Ocean. Major horizontal (sinistral) movements along the northeast– southwest axis of the adjacent Benue Trough appear to have been translated to the north-south and northwesterly trending shear zones to form the Mid-Niger Basin perpendicular to the Benue Trough (Benkhelil, 1989). Although the sedimentary fill of the Benue Trough consists of three unconformity-bounded depositional successions (Petters, 1978), the Bida and Anambra geographical regions were platforms until the Santonian. Pre-Santonian sediments are recorded

principally in the older Benue Trough and parts of the southern Anambra Basin. The collapse of the Mid-Niger and Anambra platforms led to the sedimentation of the Upper Cretaceous depositional cycle commencing with the fully marine shales of the Campanian Nkporo and Enugu Formations which may have some lateral equivalents in the Lokoja Formation of the Bida Basin. Overlying the Nkporo Formation is the sedimentary units of the Mamu Formation. These consist of shales, siltstones, sandstones and coals of fluvio-deltaic to fluvio-estuarine environments whose lateral equivalents are the conglomerates, cross-bedded and poorly sorted sandstones and claystones of the Lokoja and Bida Formations in the Bida Basin.

The Mamu Formation is succeeded by sandstones of the Lower Maastrichtian Ajali Formation laterally equivalent to the Patti, Sakpe and Enagi Formations of the Bida Basin. These sandstones are well sorted, quartz arenite that are commonly interbedded with siltstones and claystones and similar in part to the lithologies of the Patti and Enagi Formations. The Patti and Enagi Formations are overlain by the Agbaja and Batati Formations (lateral equivalents) of Upper Maastrichtian age. These consist of oolitic, pisolitic and concretionary ironstones deposited within a continental to shallow marine setting. The Upper Cretaceous sedimentary sequences in the Bida Basin suggest that fully marine conditions was not established compared with the initial marine sedimentation established for the Campanian Nkporo Formation in the adjacent Anambra Basin during that transgressive cycle. A comparison of the sediment thicknesses in the two basins indicate that the successions of the Anambra Basin reached up to 8 km thickness compared with an average of 3.4 km sediment thickness in the Bida Basin (Akande and Erdtmann, 1998).

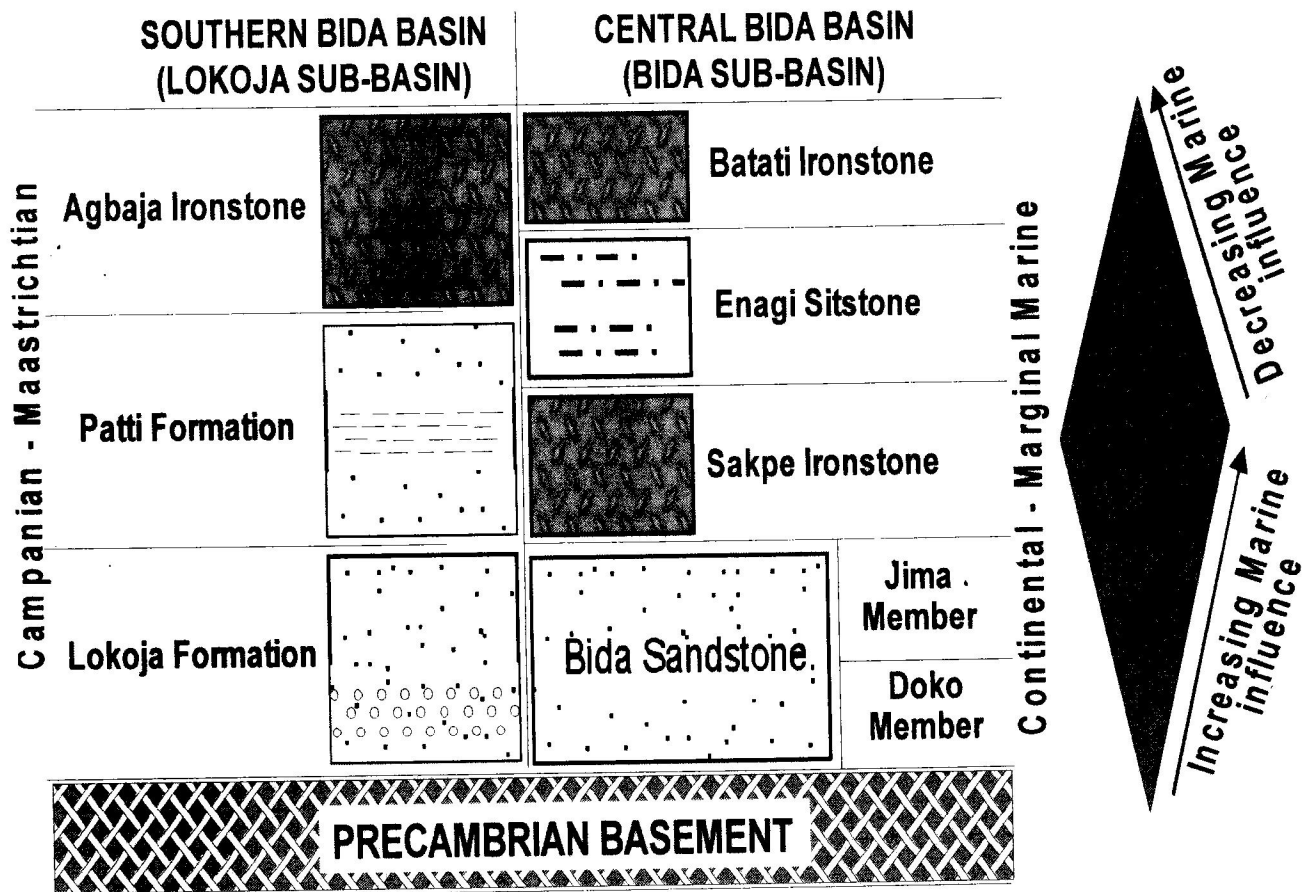


Fig. 2.1: Stratigraphy of Bida Basin (Modified from Akande et. al, 2005).

**CHAPTER THREE**  
**MATERIALS AND METHODS**

**3.1 Materials**

**Compass clinometer:** This is an instrument that indicates directions, typically by means of a freely-turning needle pointing to magnetic north. It is also used to determine the dip strike of a rock or outcrop before traversing i.e. the general rock trend.

**Chisel:** A handheld tool consisting of a solid, heavy metal which is used in chipping out hard materials, it is usually hit by a hammer. It typically drills into the hard material and chips it out.

**Hammers:** A handheld tool consisting of a solid, heavy metal which is used in hitting hard and compacted materials. The handle is usually light and it is made of wood/plastic and in some cases metal. The metal head weighs about 2kg.

**Global Positioning System (GPS):** This is used to pinpoint the longitudinal and latitudinal coordinates of the study area as well as the elevation.

**Measuring Tape:** Is a round narrow band of woven fabric, which is used for linear measurement, each measuring tape is about 50m long.

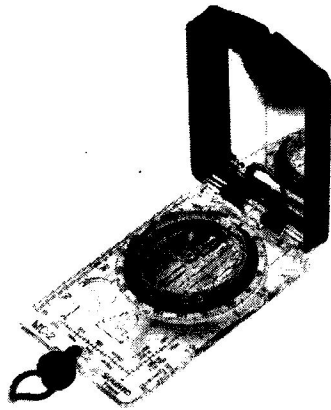


Plate 3.1: Compass

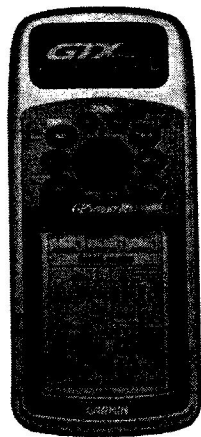


Plate 3.2: A GPS



Plate 3.3: A Geological Hammer



Plate 3.4: Chisel

### **3.1.2 Methods**

The methods employed in this study were field mapping and laboratory analyses. The field work involved outcrop description, logging of the outcrop, measurement of beds' thickness and sample collection. Bedding characteristics in terms of texture and lithology were studied in the field. Data, such as elevation, Longitude and Latitude of each location were collected using the GPS (Global Positioning System). The strike and dip of the underlying basement rock was measured using the compass clinometer and Images of outcrops and the structures on them were also taken using the Camera. The Outcrops at each locations were logged using the diameter of each bed within the sequence and described using their mineralogical, structural and textural characteristics.

Laboratory investigations of samples included pebble morphometry, grain size analysis, petrography, heavy mineral analysis and geochemical analysis. Sandstone samples were collected from Lokoja and environs which is in the Bida basin. Pebbles were picked randomly beneath the pebbly beds at outcrops studied. Each sample was divided into 4 parts: One part for grain size analysis, another for petrographic studies and the third part for heavy mineral analysis.

#### **3.2.1 Field mapping and Sample Collection**

The field work was done in the month of January, and it was done in areas in Lokoja. Three outcrops were studied in this work which is located in Filele at the outskirts of Lokoja town. The major formation encountered was the Lokoja formation which majorly consists of sandstone beds which are fluvial. Most of the outcrops were road cuts which represent the different lithofacies of the formation.

A geological hammer used in chipping, breaking and taking rock samples is the basic tool in sample materials. A chisel is employed to support the hammer to create fractures in the rock for easy breakage. A Global Positioning System (GPS) was used in taking accurate reading of the longitude and latitude and the geographic positions of outcrops on the field. A field notebook is used to record various sample locations and representation of geological information on the field and representation of the lithologic section of each sample locations were drawn. A digital camera was used in taking pictures of these rocks in-situ and interesting features to serve as back up memory in addition to the field notebook. Based on the in situ observations, textural and compositional studies of the outcrop, tentative names were given to rock samples taken from the

outcrop. Attempts were also made to determine the geologic history to explain the sequence of events as it affect rocks in the area. Finally, samples were taken with the aid of sledge hammer, a sample bag is then used to carry properly labeled samples, which were taken for petrographic preparation and other analysis. Exposed stratigraphic sections at Filele were logged accordingly and beds were identified based on sediment grain sizes and textures, colour and sedimentary structures. The logging was carried out with the aid of a measuring tape extended from bottom to top of each bed and recorded at intervals keeping into cognisance the forward extension of each bed so as to obtain the accurate thickness.

### **3.2.2 Processing and analyses of the Samples**

The laboratory study involved pebble morphometry, petrography, grain size analysis, heavy mineral analysis and Geochemical analysis. The prepared thin sections were examined under the petrological microscope to identify mineral assemblages. The optical properties of minerals such as colour, cleavage, relief etc, under plane polarized light (PPL) and birefringence, extinction under cross polarized light (XPL) also studied. Detailed description of the mineral composition and textural characteristics were interpreted.

### **3.2.3 Pebble Morphometry**

One hundred and forty-two pebbles pebbles were picked randomly beneath the pebbly beds at outcrops studied. The samples were washed carefully and numbered. Broken pebbles were removed. The three (Long, L; Intermediate, I and Short, S) axes of about one hundred and forty-two pebbles from the two locations were measured with vernier calipers. Other relevant data were computed from the gene. Some of the computed data includes indices such as: Flatness Ratio (FR), which is the ratio between the short axes to the long axes, and Elongation Ratio (ER); which is the ratio of the short to the intermediate axis. The measure of equidimensionality (sphericity) of the pebbles was determined using the Maximum Projection Sphericity Index (MPSI). Others including, the Oblate Prolate index (OPI) and Roundness were estimated. Oblate Prolate (OP) index shows how close the intermediate (I) axis of a pebble is to the short axis or long (L) axis. Roundness, which is the estimation that counts the percentage of convex parts of a pebble along its external circumference, was estimated with the aid of the charts of Sames (1966).

Roundness is a poor indicator of depositional environment, Sneed and Folk (1958) observed that pebble roundness increased downstream from river to beaches , roundness of less than 35%



typifies fluvial environment while roundness of more than 45% characterizes littoral environments. The average roundness value of the pebbles from the study area is  $45.5\% \pm 24.6$ , and, with 70% of the pebble suite having roundness varying from 20 – 43%. This result strongly suggests a fluvial environment of deposition.

#### **3.2.4 Techniques for preparation of thin section**

In the laboratory, a total of eight rock samples were selected and cut into slices with a micro-cutting machine. Field studies require integration of content, knowledge, observation and interpretation, analysis, experiment and theory and all their representations. All need to come together to form a coherent internally consistent interpretation. Thin sections were prepared for six of the collected samples during the exercise in order to carry out the petrographic study. The selected samples were cut with a micro-cutting machine into slices of 3 to 4mm, these cut samples were polished on a glass plate using carborundum.

After polishing, the samples were subjected to immense heat at a temperature of about  $80^{\circ}$  to  $90^{\circ}\text{C}$  after which a small quantity of aradite is added to the heated sample. Prior to mounting on a glass slide with aradite, the thin perfectly smooth surface rock samples air bubbles and impurities were removed.

The prepared thin section were examined under a petrological microscope to identify the mineral assemblage, morphology and other properties while the minerals optical properties such as cleavage colour, relief etc. were studied under a Plane polarized Light (PPL) and Cross Polarized light (XPL) of the petrological microscope. The results attained from these analyses were subjected to interpretation to delineate the texture, mineralogical, and modal composition of the rock types being analyzed. The slides were and studied with the aid of a petrological microscope at the laboratory of the Department of Geology, Federal University Oye-Ekiti.

#### **3.2.5 Granulometric Analysis**

A total of 12 samples were subjected to grain size analysis, the Standard grain size analysis test determines the relative proportions of different grain sizes as they are distributed among certain size ranges.

Grain size distribution is one of the most important characteristics of sediment. This is true because grain size is a powerful tool for describing a sites geomorphic setting, interpreting the geomorphic significance of fluid dynamics in the natural environment, and distinguishing local versus regional sediment transport mechanisms as well as because grain size is a dominant

controlling factor in sediment geochemistry. Characterizing the physical properties of sediment is important in determining its suitability for various uses as well as studying sedimentary environments and geologic history.

The physical properties of sediment can be described by several parameters. Grain size is the most important of these and is the main way in which sediment (and clastic sedimentary rocks) is classified. Other commonly used properties of sediment are sorting and shape (roundness and sphericity).

**Apparatus Required:**

- i. Stack of Sieves including pan and cover
- ii. Balance (with accuracy to 0.01 g)
- iii. Rubber pestle and Mortar (for crushing the soil if lumped or conglomerated)
- iv. Mechanical sieve shaker

**Test Procedure:**

- i. Take a representative oven dried sample of soil that weighs about 500g. (This is normally used for soil samples, the greatest particle size which is 4.75mm).
- ii. If soil particles are lumped or conglomerated, crush the lump and not the particles using the pestle and mortar.
- iii. Determine the mass of the sample accurately.  $W_1$  (g).
- iv. Prepare a stack of sieves. Sieves having larger openings (i.e lower numbers) are placed above the ones having smaller opening sizes (i.e higher numbers). The very last sieve is #200 and a pan is placed under it to collect the portion of soil passing #200 sieve.
- v. Make sure the sieves are clean, if many soil particles are stuck in the openings try to poke them out using brush.
- vi. Weigh all sieves and the pan separately.
- vii. Pour the soil from step 3 into the stack sieves from the top and place the cover, put the stack in the sieve shaker and fix the clamps, adjust the time on 10 to 15 minutes and get the shaker going.
- viii. Stop the sieve shaker and measure the mass of each sieve + retained soil.
- ix. The data derived are then recorded in a table.

### 3.2.6 Geochemical Analysis (XRF)

The type of geochemical method employed in this study is the X-ray Fluorescence method. Five samples were analysed in this test. For XRF measurements a sample has to be additionally pulverized, homogenized and pressed into pellet with or without a binder. Usually chromatographic cellulose, boric acid or starch are used as a binder in a proportion 1:10 by weight (in some cases a liquid binder might be used). For the emission—transmission method usually a 150 or 200 mg pellet is prepared (25 mm diameter). Although XRF is mostly used for minor and trace element analysis, major elements can be determined after proper dilution with cellulose or starch (in a proportion 1:1 by weight). Even simple sample preparation needs to be done carefully and with the use of proper devices to prevent contamination. Therefore the devices such as mills, mortars and pulverizers should be made of agate, silicon carbide or tungsten carbide. They should be washed thoroughly with tap water, then distilled water and dried. For more complete cleaning, grinding with pure quartz sand, followed by careful washing with tap and distilled water should be applied.

When dealing with samples containing heavy elements in a light (low density) matrix, which is often the case in geological samples analysis, the grain size effect can be an additional source of error in XRF analysis. The way of minimizing this effect is reduction of particle size by grinding. However, different particle size reduction occurs in most grinding procedures because the various constituents are reduced in size at different rates due to their differences in hardness, which may result in segregation. When diluents are added prior to pressing, a sample has to be mixed carefully to avoid segregation. A number of Teflon or Teflon-coated devices for homogenization are commercially available. In analysis of powdered materials, usually thick or intermediate samples are used. Thin samples are sometimes applied with the use of so-called "slurry" technique, for very fine powder (below 10 micrometer size). This technique works for water insoluble materials. A water slurry is prepared out of a few milligrams of powder and a few milliliters of water. A turbulent suspension is made followed by rapid filtration through a Nuclepore filter. This method results in fairly uniform thin layers and is applied in XRF. In the analysis of particular geological materials, and soil when concentrations of trace elements are to be determined, wet digestion might be applied.

## CHAPTER FOUR

### RESULTS AND DISCUSSIONS

#### 4.1 Lithostratigraphy

Lithologic units in the study area range from conglomerates, coarse to medium grained sandstones in the Lokoja area. Angular to Sub-angular cobbles, pebbles and granule sized quartz grains in the units are frequently distributed. The Lokoja Formation lies unconformably on the Precambrian Basement Complex. The contact between the Lokoja Formation and the basement mapped in this study is visible at Filele along the Okene-Lokoja express way (Fig. 4.1). The proximity of the sediments to the Precambrian basement in this area accounts for the arkosic components which have been derived from the disintegration of granitic rock fragments plucked from the adjoining basement. High angle cross bedding, fining-upward sequences underlain by very poorly sorted, medium to cobbly conglomeratic sands with large quartzite breccias interpreted as channel lag deposits, characteristic of point bar deposits is commonly exhibited.



Fig. 4.1: The Lokoja Formation exposed at Filele 1(Long.  $07^{\circ} 51' 18''$  E, Lat.  $006^{\circ} 41' 54.5''$  N)



Fig. 4.2: The Lokoja Formation exposed at Filele 2 (Long.  $06^{\circ} 042^1 43^{11}E$ , Lat.  $07^{\circ} 51^1 15.0^{11}N$ )



Fig. 4.3: The Lokoja Formation exposed at Filele 3.(Lat.  $07^{\circ} 51' 11''$ N, Long.  $06^{\circ} 42' 59''$ E)

### **Lithologic description**

The first outcrop is located at Long.  $07^{\circ} 51' 18''$  E, Lat.  $006^{\circ} 41' 54.5''$  N with an elevation of 160m. The outcrop has four beds of different lithologic unit starting from the base with the weathered basement (Gneiss) 1.4m, unconformably overlying the weathered basement is the conglomeratic sandstone which is Cross stratified with a thickness of 2.6m, overlying it is 1.4m thick massive conglomeratic sandstone, which is then overlain by a reddish massive conglomeratic sandstone which is 4m thick. The beds in successions have a total thickness of 9.4m (Fig. 4.5).



TH (m)	LITHOLOGY					SAMPLE NO	DESCRIPTION
	Clay	Silt	Sand	Granule	Pebble		
9.4						FE1E	reddish massive conglomeratic sandstone
5.4						FE1D	Milky massive conglomeratic sandstone
4.0						FE1C	Trough cross stratified conglomeratic sandstone
1.4						FE1B	Erosional sandstone
						FE1A	Basement (Gneiss)

Fig. 4.4: Litholog of Filele 1 outcrop (Long. 07° 51' 18<sup>11</sup> E, Lat. 006° 41' 54.5<sup>11</sup> N)

The second outcrop is located at Long.  $06^{\circ} 042' 43''$ , Lat.  $07^{\circ} 51' 15.0''$  with an elevation of 142m. The outcrop has five beds of different lithologic units, the oldest being a quartz, feldspar, muscovite rich stratified medium grained sandstone which is 1.3m thick, essentially overlying this bed is a massive milky sandy claystone which is about 1m thick. Graded bedded conglomeratic sandstone can be seen to overlay the second bed and it is about 2.95m thick, a ferruginized sandstone bed is overlying the third bed (0.6m). The youngest bed in this area is an Oolitic ironstone bed which is about 1m thick. (Fig. 4.6).

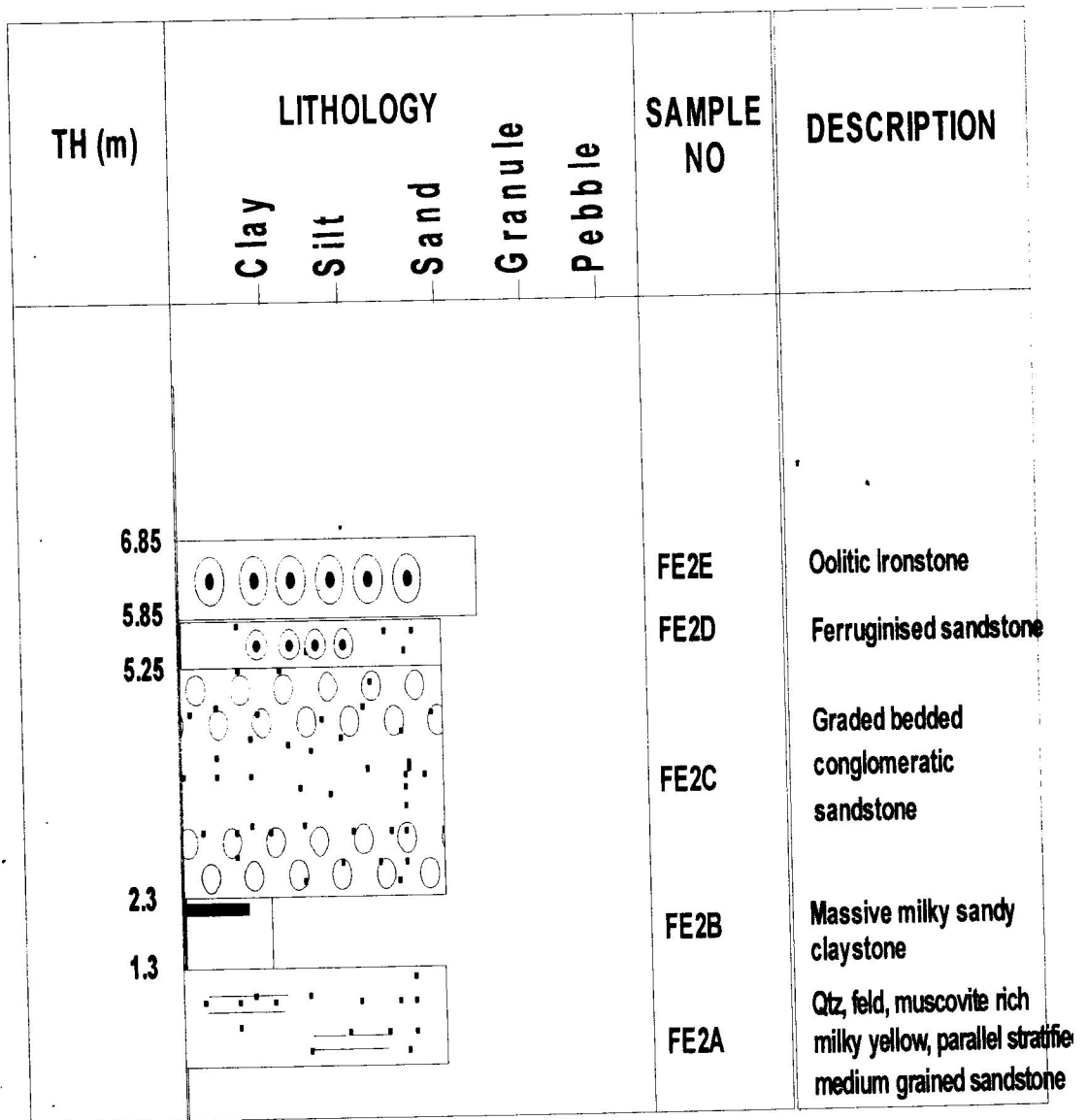


Fig. 4.5: Litholog of Filele 2 outcrop (Long.  $06^{\circ} 042^1 43^{11}$ , Lat.  $07^{\circ} 51^1 15.0^{11}$ )

The Third outcrop is located at Lat.  $07^{\circ} 51' 11''$ N and Long.  $06^{\circ} 42' 59''$  E with an elevation of 95m. The outcrop has five beds of different lithologic units. The first bed is a massive milky pebbly coarse grained sandstone which is about 0.7m thick. Overlying this bed is a massive medium to fine grained sandstone which is essentially about 2m thick. Overlying this bed is a massive matrix supported conglomeratic bed about 3.92m thick. A fine to medium grained sandstone is seen to overlie the previous bed and it is about 1m thick. The youngest bed in the area is a massive matrix supported conglomerate bed and it is about 4.5m thick. (Fig. 4.7).

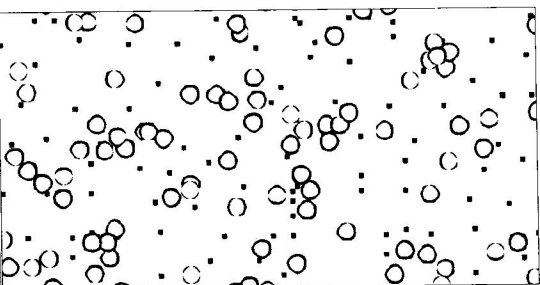

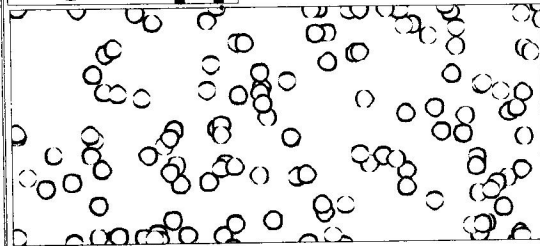


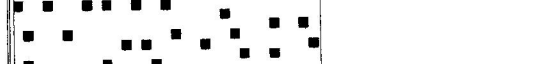

TH (m)	LITHOLOGY					SAMPLE NO	DESCRIPTION
	Clay	Silt	Sand	Granule	Pebble		
13.13						FE3G	Massive matrix supported Conglomerate
8.63						FE3F	Fine to medium grained sandstone
7.63						FE3E	Massive matrix supported conglomerate
3.71						FE3D	Massive fine grained sandstone
3.23						FE3C	Fine-medium grained sandstone
2.03						FE3B	Massive brownish clayey medium grained sandstone
0.7						FE3A	Massive milky pebbly coarse grained sandstone

Fig. 4.6: Litholog of Filele 3 outcrop. (Lat.  $07^{\circ} 51' 11''$ N, Long.  $06^{\circ} 42' 59''$  E)

## 4.2 Texture

### 4.2.1 Pebble Morphometry

Pebbles were picked randomly within the pebbly beds at both of the conglomeratic sandstone outcrops studied, the three axes the Long (L), Intermediate (I), and the short (S) were measured for three set(s) of quartzite pebbles, at the first, second 60, 70 and 18 pebbles were picked randomly. The samples were washed carefully and numbered. Broken pebbles were removed, and this was done at the Geology laboratory of Federal University Oye-Ekiti. One hundred and forty-two pebbles from the two locations were measured with vernier calipers. Other relevant data were computed from the gene. Some of the computed data includes indices such as: Flatness Ratio (FR), which is the ratio between the short axes to the long axes, and Elongation Ratio (ER), which is the ratio of the short to the intermediate axis. The measure of equidimensionality (sphericity) of the pebbles was determined using the Maximum Projection Sphericity Index (MPSI). Others including, the Oblate Prolate index (OPI) and Roundness were estimated. Oblate Prolate (OP) index shows how close the intermediate (I) axis of a pebble is to the short axis or long (L) axis. Roundness, which is the estimation that counts the percentage of convex parts of a pebble along its external circumference, was estimated with the aid of the charts of Sames (1966).

The results obtained from the morphometric analysis of pebbles from the Lokoja formation is presented in Table 4.2, 4.3 and 4.4, while Table 4.5 contain the summary of morphometric data, characteristics and environmental diagnosis for the pebble morphometric analysis. As shown in Table 4.5, the mean flatness ratio (FR) for the pebbles from Lokoja Formation is  $0.61 \pm 0.12$ . Similarly, elongation ratio (ER) has mean value of  $0.69 \pm 0.12$ , and roundness has values ranging from 30% to 70% with mean value of 37.6%. The mean maximum projection sphericity index (M.P.S.I) for pebbles from the Lokoja Formation is  $0.81 \pm 0.06$ . The Oblate – Prolate index values ranges from  $1.62 \pm 0.65$ . Roundness is a poor indicator of depositional environment, Sneed and Folk (1958) observed that pebble roundness increased downstream from river to beaches, roundness of less than 35% typifies fluvial environment while roundness of more than 45% characterizes littoral environments. The average roundness value of the pebbles from the study area is  $35.73\% \pm 7.137$  and 60% of the pebble having roundness varying from 20 – 45%. This result very much implies a fluvial depositional environment.

**Table 4.1:** Computed and Estimated Morphometric Properties Used in the study

Morphometric Indices	Formula	Author
Flatness Ratio (F.R)	S/L	Lutig (1962)
Elongation Ratio (E.R)	I/L	Lutig (1962)
Maximum Projection Sphericity Index (M.P.S.I)	$(S^2/LI)^{1/3}$	Sneed and Folk (1958)
Oblate - Prolate (OP) Index	$10[(L-I/L-S)-0.50]S/L$	Dobkins and Folk (1970)
Roundness	Visual estimation	Sames (1966)

**Table 4.2:** Morphometric Data of Lokoja Formation Pebbles from Filele (FE1E)

	L	I	S	S/L	S/L*100	I/L	I-I/L-S	SPHERICITY	OP INDEX	ROUNDNESS
	5.50	4.65	2.40	0.436	43.636	0.845	0.274	0.608	-5.175	40
	5.90	4.70	4.00	0.678	67.797	0.797	0.632	0.833	1.941	35
	2.70	2.25	2.00	0.741	74.074	0.833	0.643	0.870	1.929	30
	3.50	2.90	2.50	0.714	71.429	0.829	0.600	0.851	1.400	35
	4.65	3.00	2.30	0.495	49.462	0.645	0.702	0.724	4.086	40
	3.80	3.00	1.90	0.500	50.000	0.789	0.421	0.682	-1.579	30
	3.90	3.00	2.60	0.667	66.667	0.769	0.692	0.833	2.885	30
	3.60	2.00	1.80	0.500	50.000	0.556	0.889	0.766	7.778	30
	5.40	2.50	2.60	0.481	48.148	0.463	1.036	0.794	11.126	40
	5.50	4.30	2.80	0.509	50.909	0.782	0.444	0.692	-1.091	30
	5.80	3.60	2.70	0.466	46.552	0.621	0.710	0.704	4.504	30
	5.80	3.70	2.40	0.414	41.379	0.638	0.618	0.645	2.843	30
	4.60	3.60	2.70	0.587	58.696	0.783	0.526	0.761	0.448	30
	3.30	2.30	2.40	0.727	72.727	0.697	1.111	0.912	8.403	35
	3.30	2.80	1.30	0.394	39.394	0.848	0.250	0.568	-6.346	40
	2.90	2.50	1.30	0.448	44.828	0.862	0.250	0.615	-5.577	45
Av.	4.384	3.175	2.356	0.547	54.731	0.735	0.612	0.741	1.723	34.375
St. Dev.	1.135	0.842	0.641	0.116	23.497	0.115	0.247	0.100	4.823	5.123

Table 4.3: Morphometric Data of Lokoja Formation Pebbles from Filele (FE2C)

L	l	s	S/L	S/L*100	l/L	L-l/L-S	SPERICITY	OP INDEX	ROUNDNESS
5.30	5.00	4.90	0.925	92.453	0.943	0.750	0.968	2.704	40
3.15	2.45	2.00	0.635	63.492	0.778	0.609	0.803	1.712	30
7.40	3.40	3.10	0.419	41.892	0.459	0.930	0.726	10.270	40
4.75	3.60	3.20	0.674	67.368	0.758	0.742	0.843	3.581	40
4.40	3.30	3.00	0.682	68.182	0.750	0.786	0.853	4.190	40
5.40	3.20	2.95	0.546	54.630	0.593	0.898	0.796	7.285	45
5.40	4.00	3.50	0.645	64.815	0.741	0.737	0.828	3.654	40
4.90	3.70	3.25	0.663	66.327	0.755	0.727	0.835	3.427	30
4.90	2.90	2.50	0.510	51.020	0.592	0.833	0.760	6.533	30
5.90	3.25	3.00	0.508	50.847	0.551	0.914	0.777	8.138	35
6.20	4.70	4.40	0.710	70.968	0.758	0.833	0.873	4.697	40
4.60	2.85	2.50	0.543	54.348	0.620	0.833	0.781	6.133	45
3.80	3.50	3.10	0.816	81.579	0.921	0.429	0.897	-0.876	50
6.10	3.80	3.40	0.557	55.738	0.623	0.852	0.793	6.313	35
5.70	4.20	3.90	0.684	68.421	0.737	0.833	0.860	4.872	30
3.80	2.95	2.50	0.658	65.789	0.776	0.654	0.823	2.338	40
3.65	2.70	2.60	0.712	71.233	0.740	0.905	0.882	5.682	40
3.95	2.90	2.50	0.633	63.291	0.734	0.724	0.817	3.541	30
3.90	2.80	2.65	0.679	67.949	0.718	0.880	0.863	5.582	40
8.20	5.85	5.60	0.683	68.293	0.713	0.904	0.868	5.913	30
5.00	4.25	4.00	0.800	80.000	0.850	0.750	0.910	3.125	35
5.50	3.50	3.20	0.582	58.182	0.636	0.870	0.810	6.352	30
4.70	3.50	3.10	0.660	65.957	0.745	0.750	0.836	3.790	30
5.10	3.10	2.80	0.549	54.902	0.608	0.870	0.792	6.731	30
4.90	3.10	2.60	0.565	56.522	0.674	0.750	0.780	4.423	30
5.10	2.80	2.40	0.471	47.059	0.549	0.852	0.739	7.477	40
4.10	2.90	2.20	0.537	53.659	0.610	0.842	0.779	6.376	35
4.50	2.90	2.60	0.578	57.778	0.644	0.842	0.805	5.921	40
3.45	2.20	1.85	0.536	53.623	0.638	0.781	0.767	5.245	45
4.90	3.10	2.70	0.551	55.102	0.633	0.818	0.783	5.774	35
4.10	2.80	2.50	0.610	60.976	0.683	0.813	0.817	5.125	30
3.90	2.60	2.10	0.538	53.846	0.667	0.722	0.758	4.127	30
3.40	2.80	2.60	0.765	76.471	0.824	0.750	0.892	3.269	30
3.20	2.60	2.40	0.750	75.000	0.813	0.750	0.885	3.333	45
3.80	2.40	2.10	0.553	55.263	0.632	0.824	0.785	5.854	45
3.90	2.45	2.10	0.538	53.846	0.628	0.806	0.773	5.675	40
8.70	4.60	4.15	0.477	47.701	0.529	0.901	0.755	8.409	30
5.30	3.20	2.80	0.528	52.830	0.604	0.840	0.773	6.436	30
4.75	2.30	1.90	0.400	40.000	0.484	0.860	0.691	8.991	45
3.40	2.60	2.30	0.676	67.647	0.765	0.727	0.843	3.360	30
5.00	2.20	1.75	0.390	39.000	0.440	0.862	0.633	10.330	35
3.40	2.40	2.10	0.618	61.765	0.706	0.769	0.815	4.359	40
4.90	4.20	3.95	0.806	80.612	0.857	0.737	0.912	2.938	40
4.70	3.30	3.00	0.638	63.830	0.702	0.824	0.834	5.069	30
4.10	3.00	2.80	0.683	68.293	0.732	0.846	0.881	5.069	30
3.60	3.20	2.90	0.806	80.556	0.889	0.571	0.900	0.887	40
4.00	2.35	2.10	0.525	52.500	0.588	0.868	0.777	7.018	35
3.60	2.20	1.95	0.542	54.167	0.611	0.848	0.783	6.434	30
3.60	2.20	1.80	0.500	50.000	0.611	0.778	0.742	5.556	40
4.10	2.60	2.40	0.585	58.537	0.634	0.882	0.814	6.532	30
3.65	2.45	2.10	0.575	57.534	0.671	0.774	0.790	4.766	30
3.40	2.80	2.60	0.765	76.471	0.824	0.750	0.892	3.269	40
3.70	2.85	2.55	0.689	68.919	0.770	0.739	0.851	3.470	45
3.60	2.55	2.30	0.639	63.889	0.708	0.808	0.832	4.816	40
3.50	3.00	2.80	0.800	80.000	0.837	0.714	0.907	2.679	40
3.70	3.10	2.65	0.716	71.622	0.838	0.571	0.849	0.997	30
4.05	1.30	1.10	0.272	27.160	0.321	0.932	0.613	15.913	30
2.60	2.00	1.80	0.692	69.231	0.769	0.750	0.834	3.611	30
3.20	2.30	1.90	0.594	59.375	0.719	0.692	0.789	3.239	30
3.30	2.20	1.85	0.561	56.061	0.667	0.759	0.778	4.613	30
3.45	2.00	1.75	0.907	90.725	0.580	0.853	0.763	6.958	35
2.65	2.40	2.10	0.792	79.245	0.906	0.455	0.885	-0.574	35
2.70	2.20	1.90	0.704	70.370	0.815	0.625	0.847	1.776	30
3.40	2.65	2.40	0.706	70.588	0.779	0.750	0.861	3.542	30
3.50	1.90	1.60	0.457	45.714	0.543	0.842	0.727	7.484	30
3.80	2.30	1.70	0.447	44.737	0.605	0.714	0.692	4.790	50
3.00	2.60	2.00	0.667	66.667	0.867	0.400	0.800	-1.500	40
3.60	1.50	1.30	0.361	36.111	0.417	0.913	0.679	11.438	45
AV	4.332	2.943	2.619	0.611	61.098	0.690	0.811	5.014	36.250
St Dev	1.180	0.805	0.811	0.123	12.293	0.124	0.111	0.065	6.192



**Table 4.4: Morphometric Data of Lokoja Formation Pebbles from Filele (FE1B)**

L	I	S	S/L	S/L*100	I/L	I-I/L-S	SPHERICITY	OP INDEX	ROUNDNESS	
7.90	6.90	6.50	0.823	82.278	0.873	0.714	0.919	2.604	45	
7.25	5.90	5.30	0.731	73.103	0.814	0.692	0.869	2.631	35	
7.50	6.80	6.50	0.867	86.667	0.907	0.700	0.939	2.308	30	
5.50	4.25	4.00	0.727	72.727	0.773	0.833	0.881	4.583	35	
4.10	2.40	2.20	0.537	53.859	0.585	0.895	0.789	7.356	40	
7.60	5.40	5.10	0.671	67.105	0.711	0.880	0.859	5.663	30	
7.00	4.30	4.00	0.571	57.143	0.614	0.900	0.810	7.000	35	
8.50	4.30	3.80	0.447	44.706	0.506	0.894	0.734	8.805	30	
5.25	4.20	3.90	0.743	74.286	0.800	0.778	0.884	3.739	40	
3.60	3.00	2.60	0.722	72.222	0.833	0.600	0.855	1.385	30	
6.20	4.10	4.00	0.643	64.516	0.661	0.953	0.857	7.045	30	
4.60	3.10	3.00	0.652	65.217	0.674	0.938	0.858	6.708	30	
6.40	4.90	4.50	0.703	70.313	0.766	0.789	0.864	4.117	30	
7.20	4.80	4.30	0.597	59.722	0.667	0.828	0.812	5.455	40	
3.70	2.30	1.80	0.486	48.649	0.622	0.737	0.725	4.868	40	
5.00	3.70	3.00	0.600	60.000	0.740	0.650	0.786	2.500	45	
4.60	2.90	2.50	0.543	54.348	0.630	0.810	0.777	5.695	30	
4.10	3.35	3.00	0.732	73.171	0.817	0.682	0.869	2.485	50	
5.20	3.80	3.50	0.673	67.308	0.731	0.824	0.853	4.807	40	
4.40	3.70	3.20	0.727	72.727	0.841	0.583	0.857	1.146	40	
7.10	4.00	3.80	0.535	53.521	0.563	0.939	0.798	8.210	40	
3.25	2.75	2.50	0.769	76.923	0.846	0.667	0.888	2.167	30	
3.80	3.10	3.05	0.803	80.263	0.816	0.933	0.924	5.399	40	
11.50	6.30	6.00	0.522	52.174	0.548	0.945	0.792	8.538	35	
3.60	2.60	2.25	0.625	62.900	0.722	0.741	0.815	3.852	35	
3.70	2.60	2.10	0.568	56.757	0.703	0.688	0.771	3.304	45	
3.55	2.10	1.65	0.465	46.479	0.592	0.763	0.715	5.662	40	
3.20	2.50	2.40	0.750	75.000	0.781	0.875	0.896	5.000	50	
4.20	3.30	3.10	0.738	73.810	0.786	0.818	0.885	4.311	30	
5.00	3.40	2.85	0.570	57.000	0.680	0.744	0.782	4.284	30	
4.00	3.35	3.00	0.750	75.000	0.838	0.650	0.876	2.000	40	
3.90	2.40	2.10	0.538	53.846	0.615	0.833	0.778	6.190	30	
6.80	5.40	5.00	0.735	73.529	0.784	0.778	0.880	3.778	30	
4.20	3.20	2.90	0.690	69.048	0.762	0.769	0.855	3.899	40	
4.55	3.30	2.90	0.549	54.945	0.725	0.610	0.747	1.998	40	
5.05	3.00	2.80	0.554	55.446	0.594	0.911	0.803	7.415	30	
5.20	4.10	3.65	0.702	70.192	0.788	0.710	0.855	2.987	45	
3.80	2.40	2.05	0.539	53.947	0.632	0.800	0.772	5.561	30	
2.75	2.50	1.85	0.673	67.273	0.909	0.278	0.793	-3.303	40	
5.20	3.10	2.65	0.510	50.962	0.596	0.824	0.758	6.349	40	
8.00	4.85	4.50	0.563	56.250	0.606	0.900	0.805	7.111	40	
4.50	3.60	3.20	0.711	71.111	0.800	0.692	0.858	2.704	30	
4.30	1.90	1.30	0.302	30.233	0.349	0.933	0.640	14.333	30	
5.50	2.80	2.60	0.473	47.273	0.509	0.931	0.760	9.118	40	
6.90	5.00	4.65	0.715	71.538	0.769	0.811	0.873	4.345	40	
11.40	6.20	6.00	0.526	52.632	0.544	0.963	0.799	8.796	30	
4.90	4.15	3.80	0.776	77.551	0.847	0.682	0.892	2.344	40	
3.40	2.40	1.90	0.559	55.882	0.706	0.667	0.762	2.982	30	
3.50	2.30	2.10	0.600	60.000	0.657	0.857	0.818	5.952	30	
5.20	2.20	2.00	0.385	38.462	0.423	0.938	0.704	11.375	40	
3.80	2.60	2.20	0.579	57.895	0.684	0.750	0.788	4.318	45	
3.80	2.20	1.80	0.474	47.368	0.579	0.800	0.729	6.333	40	
12.00	5.80	5.40	0.450	45.000	0.483	0.939	0.748	9.764	40	
6.85	4.50	4.10	0.599	59.854	0.657	0.855	0.817	5.924	30	
3.85	3.25	3.00	0.779	77.922	0.844	0.706	0.896	2.642	30	
3.50	2.50	2.25	0.643	64.286	0.714	0.800	0.833	4.667	30	
8.30	6.00	5.50	0.663	66.265	0.723	0.821	0.847	4.851	45	
3.40	3.00	2.50	0.735	73.529	0.882	0.444	0.849	-0.756	30	
Av.	5.391	3.696	3.340	0.626	62.613	0.701	0.784	0.821	4.920	36.293
St. Dev.	2.105	1.311	1.304	0.117	23.476	0.123	0.130	0.061	2.875	6.038

**LEGEND:** L = Long axes, I = Intermediate axes, S = Short axes, OP = Oblate - Prolate Index  
 I/L = Elongation Ratio. Sphericity = MPSI, S/L = Flatness Ratio, S/L\*100 = Coefficient of Flatness

**Table 4.5: Pebble Morphological Analysis Interpretation**

<b>Pebble morphometric parameters</b>	<b>Characteristics</b>	<b>Define limits from previous studies</b>	<b>Interpretation of Depositional Environment/ Processes</b>
<b>Flatness Index (FI)</b>	Consist of over 90% above fluvial limit	(Lutig, 1962), Beach <45%, Fluvial>45%	<i>Fluvial</i>
<b>Elongation Ratio</b>	Over 95% has values between 0.6-0.9	(Hubert, 1968), Fluvial (0.6-0.9)	<i>Fluvial</i>
<b>Maximum Projection Sphericity Index (MPSI)</b>	The pebbles analyse about 97% were above 0.66	(Dobkinsand Folk), 1970, Beach <0.66, Fluvial >0.66	<i>Predominantly Fluvial</i>
<b>Oblate Prolate Index (OPI)</b>	The OPI shows significant of fluvial deposit with minimal beach	(Sneed and Folk), 1958, Beach < -1.5, Fluvial > -1.5	<i>Fluvial Dominated</i>
<b>Roundness (R)</b>	60% has values below 0.35 and 40% has values above 0.45	(Sames, 1966), Fluvial < 0.35%, Littoral>0.45 %	<i>Mainly Fluvial/ Littoral with few beach pebbles</i>

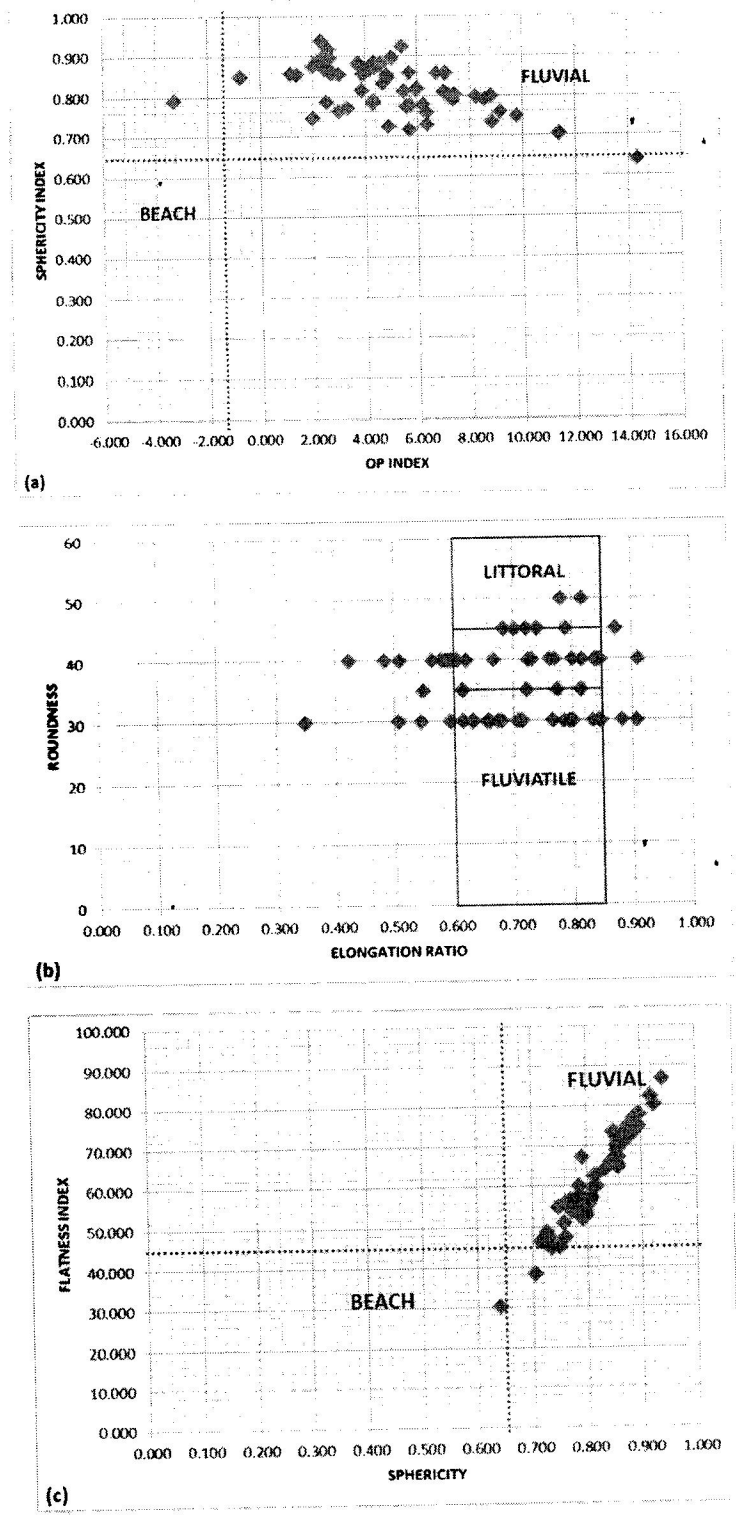
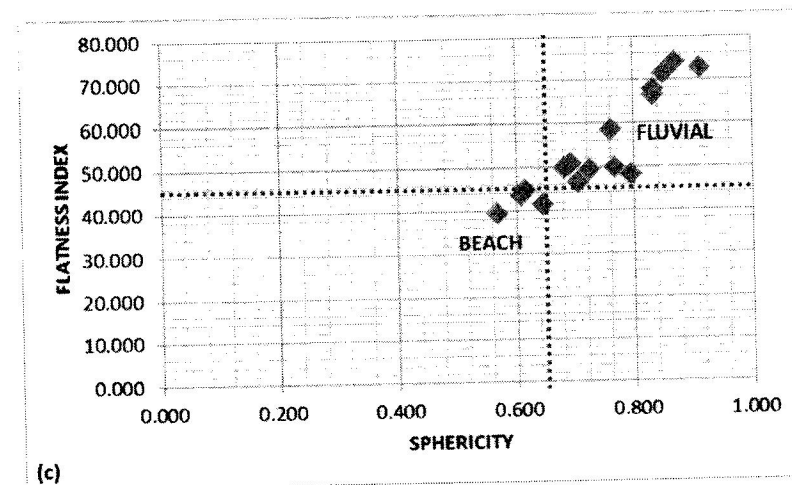
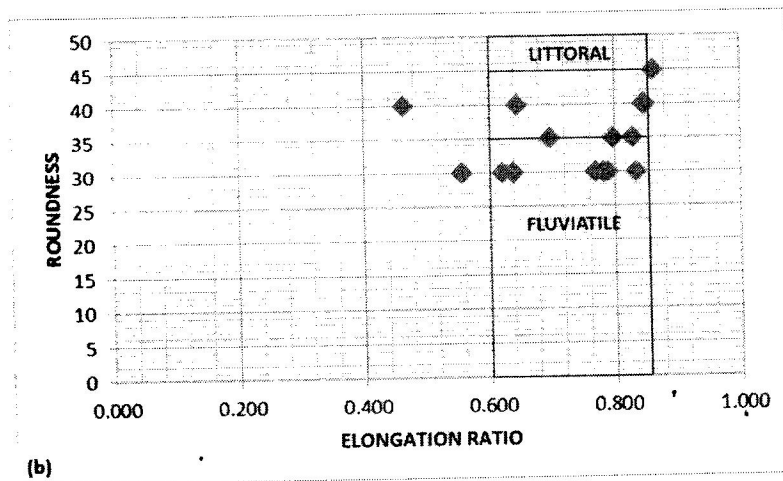
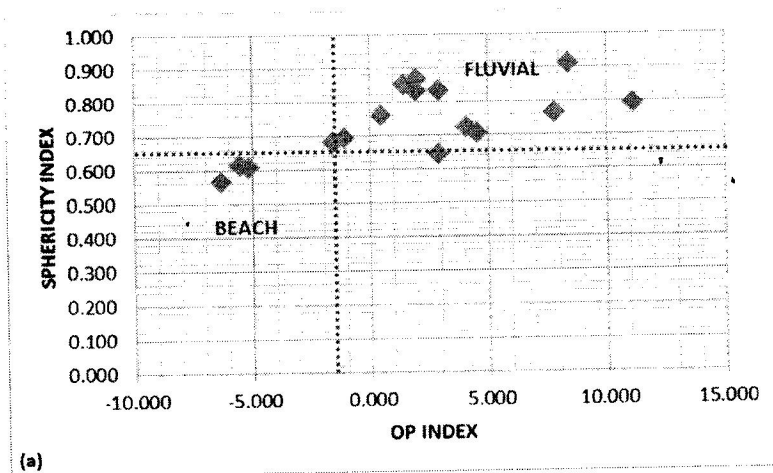


Fig. 4.7: Scattered Plots of the Pebble Forms for FE1B: (a) Plot of sphericity against OP Index showing separation of beach field from the fluvial field; (b) Plot of roundness against elongation ratio; (c) Bivariate plot of Flatness Index and Sphericity Index.



**Fig. 4.8:** Scattered Plots of the Pebble Forms for FE1E: (a) Plot of sphericity against OP Index showing separation of beach field from the fluvial field; (b) Plot of roundness against elongation ratio; (c) Bivariate plot of Flatness Index and Sphericity Index.

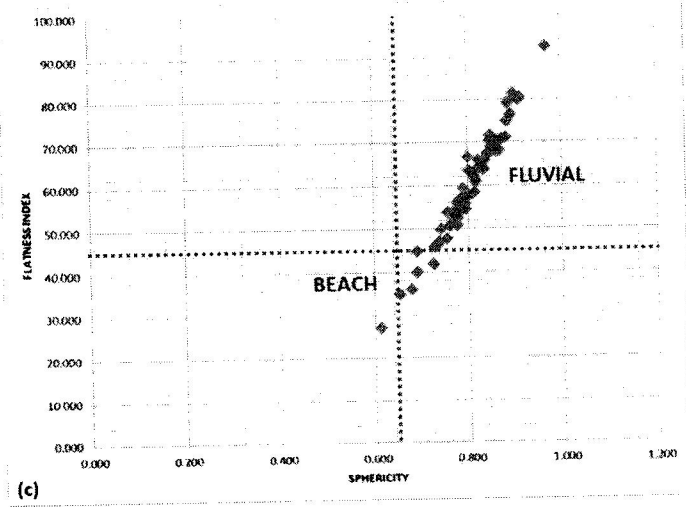
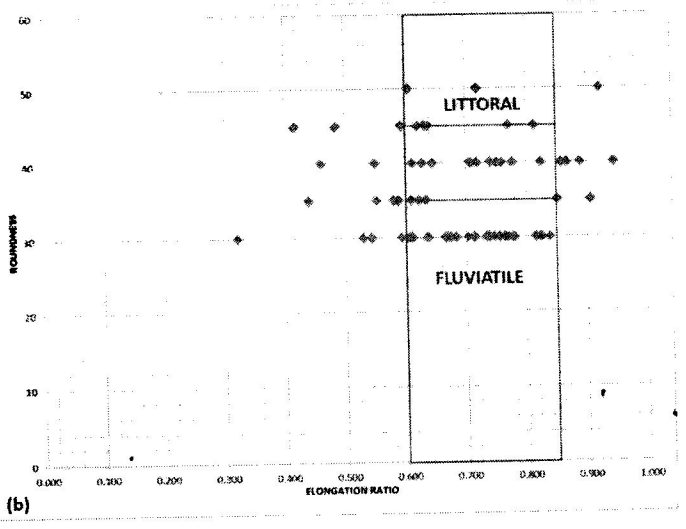
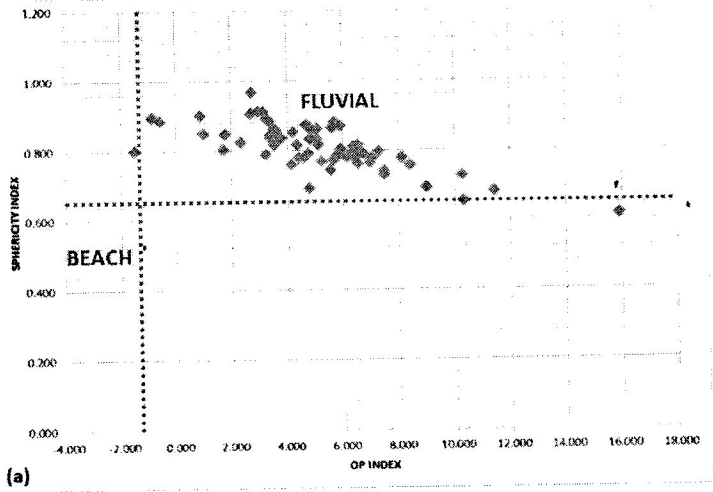


Fig. 4.9: Scattered Plots of the Pebble Forms for FE2C: (a) Plot of sphericity against OP Index showing separation of beach field from the fluvial field; (b) Plot of roundness against elongation ratio; (c) Bivariate plot of Flatness Index and Sphericity Index.

### 4.2.2 Grain size analysis

Grain size analysis was carried out at Geology laboratory of Federal University Oye-Ekiti. Twelve (12) different samples were analysed, samples from Filele. The aim of this analysis is to determine the depositional environment of the samples. The graph of Cumulative weight percent against phi size is used to determine the values for  $\phi_5$ ,  $\phi_{16}$ ,  $\phi_{25}$ ,  $\phi_{50}$ ,  $\phi_{75}$ ,  $\phi_{84}$  and  $\phi_{95}$ . These values are then substituted into the equations below to determine the graphic mean, inclusive graphic standard deviation (sorting), inclusive graphic skewness (skewness) and kurtosis of the sand sample. The table below shows the formulas for the graphic mean, sorting, skewness and kurtosis. (Table 4.6)

#### Grain Size Analysis Data

The data derived from the grain size analysis procedure were recorded in a table and graphs were plotted as cumulative % weight retained against phi ( $\phi$ ). The data generated include mean, graphic mean, standard deviation, inclusive graphic skewness and kurtosis.

**Table 4.6:** showing the formulas needed for determining the values for interpreting the data acquired.

	FORMULA USED	SOURCE
Graphic Mean	$M = \frac{\phi_{16} + \phi_{50} + \phi_{84}}{3}$	
Inclusive Graphic Standard Deviation	$D = \frac{\phi_{84} - \phi_{16}}{4} + \frac{\phi_{95} - \phi_5}{6.6}$	Folk and Ward (1957)
Graphic Skewness	$S = \frac{\phi_{84} + \phi_{16} - 2(\phi_{50})}{2(\phi_{84} - \phi_{16})} + \frac{\phi_{95} + \phi_5 - 2(\phi_{50})}{2(\phi_{95} - \phi_5)}$	
Kurtosis	$K = \frac{\phi_{95} - \phi_5}{2.44(\phi_{75} - \phi_{25})}$	

## Processing and Analyses Of The Samples

Table 4.7: Grain Size Analysis data for Filele Sandstone.

Sieve Size	CUMMULATIVE WEIGHT RETAINED (%)											
	FE1B	FE1D	FE1E	FE2A	FE2B	FE2C	FE3A	FE3B	FE3C	FE3E	FE3F	FE3G
4.000	0.3	3	12.9	0.1	0.6	12.1	2.3	0.4	0.7	6.7	0.1	9.4
3.350	0.3	4.5	13.5	0.3	0.9	13.2	2.5	1.9	0.8	9.2	0.1	10.1
2.000	3.4	14.3	16.9	1.5	3.3	20	5.7	4.6	1.3	20.8	1.4	15.3
1.180	9.5	32	27	3	8.7	32.2	13.5	13.2	3.3	35.6	4	25
0.600	47.1	67.7	60.7	12.8	23	56	41.3	28.7	34.9	64.7	9.7	52.1
0.425	67.3	78.2	75.4	29.7	39.6	69.8	60.5	39.4	58	77.7	18.7	73.3
0.150	90.9	93.1	95	84.2	83.6	93.7	90.6	80.5	91.3	96.5	88.6	95.1
0.075	96.1	94.8	98.1	97	94.9	97.9	96.7	93.7	97.4	98.9	96.5	98.2
0.063	96.7	95.2	98.7	98.1	97.2	98.7	98.1	96	98.5	99.3	97.7	98.7
PAN	97.7	98.7	99.8	99.4	99.1	99.9	99.8	99.3	99.9	99.9	99.7	99.1

The table above shows the cumulative % weight retained recorded from each samples from different sieve sizes. The data would be used to plot a cumulative graph for each of the samples as shown below;

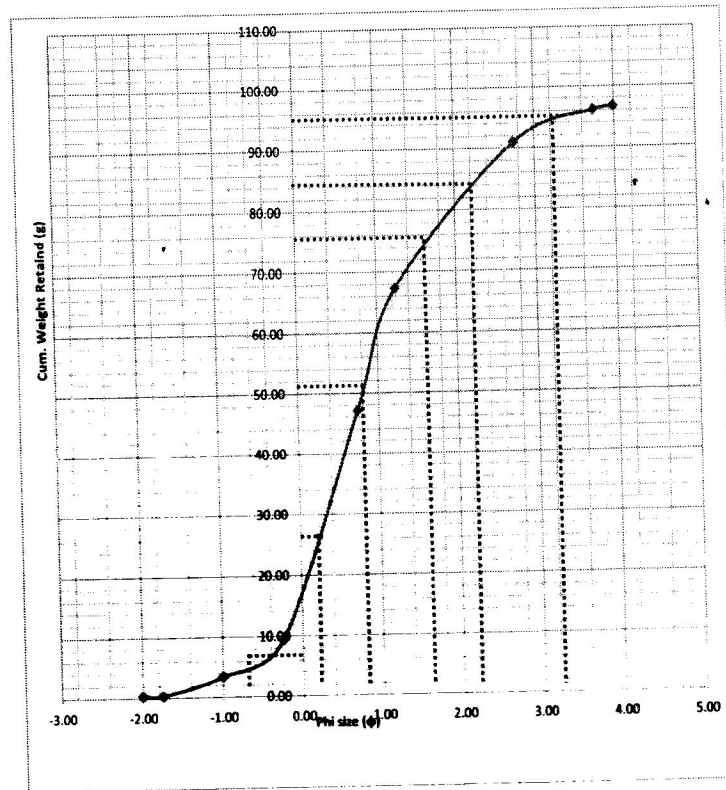


Fig. 4.10: Particle size distribution curve for sample FE1B

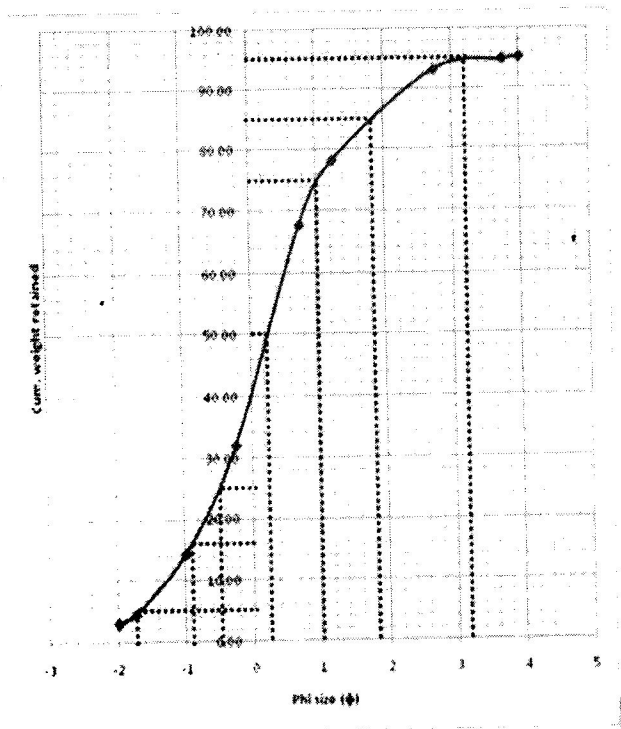


Fig. 4.11: Particle size distribution curve for sample FE1D

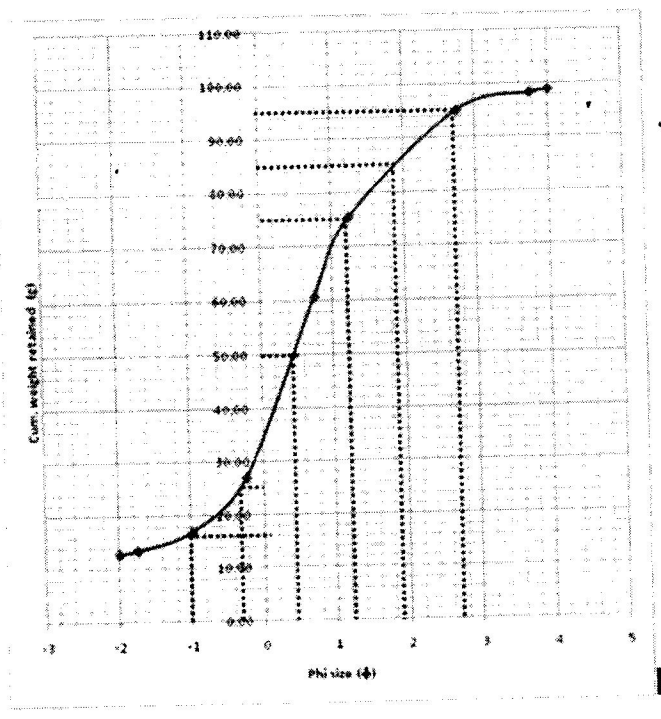


Fig. 4.12: Particle size distribution curve for sample FE1E



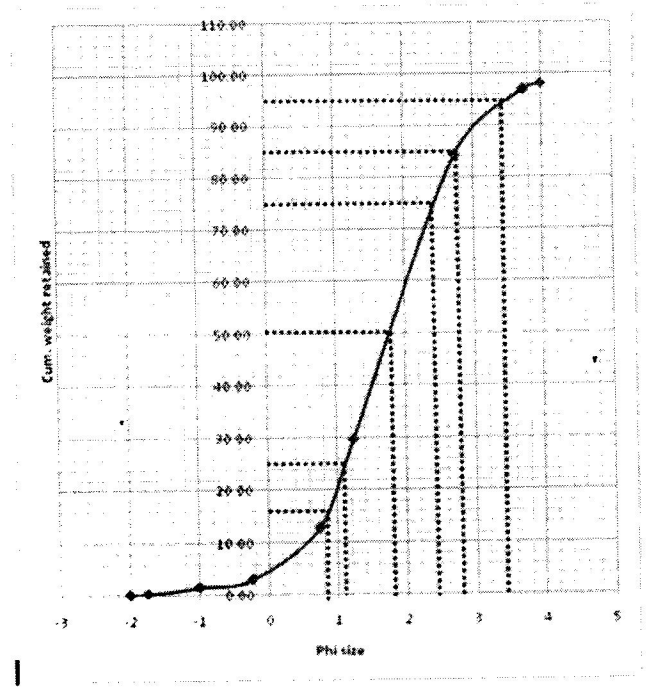


Fig. 4.13: Particle size distribution curve for sample FE2A

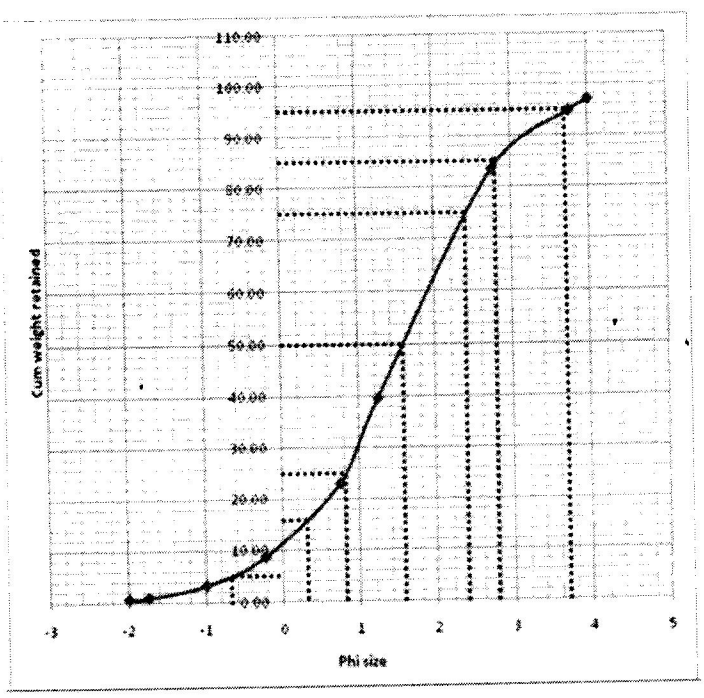


Fig. 4.14: Particle size distribution curve for sample FE2B

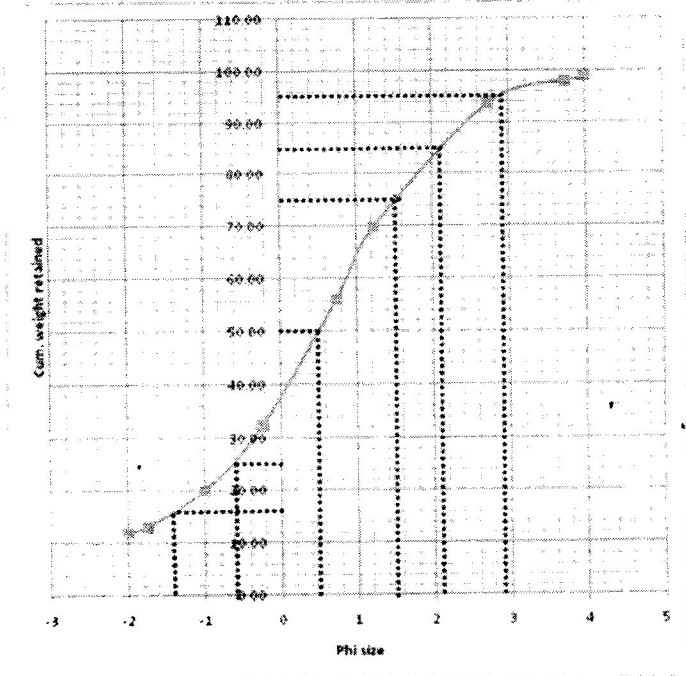


Fig. 4.15: Particle size distribution curve for sample FE2C

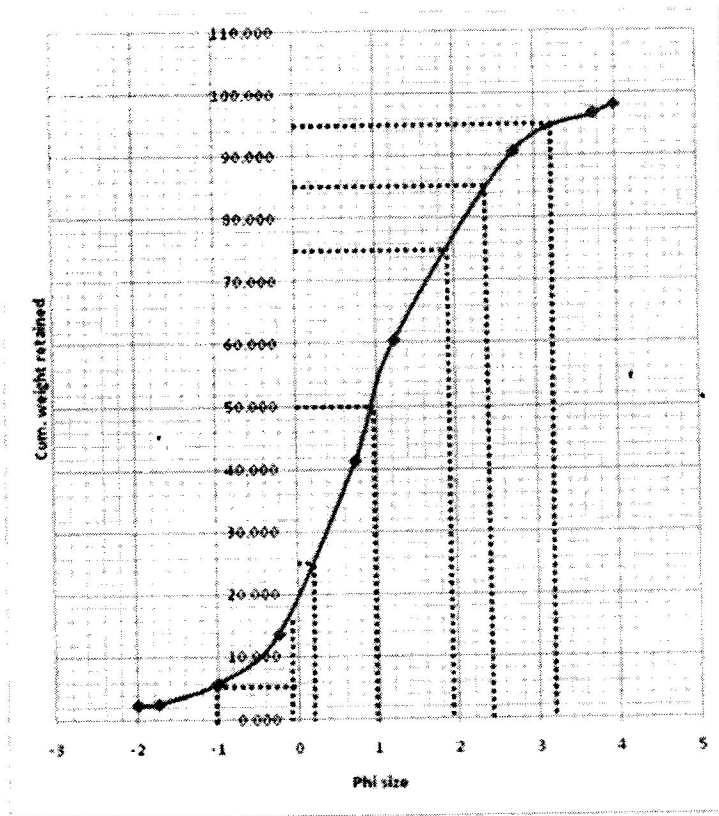


Fig. 4.16: Particle size distribution curve for sample FE3A

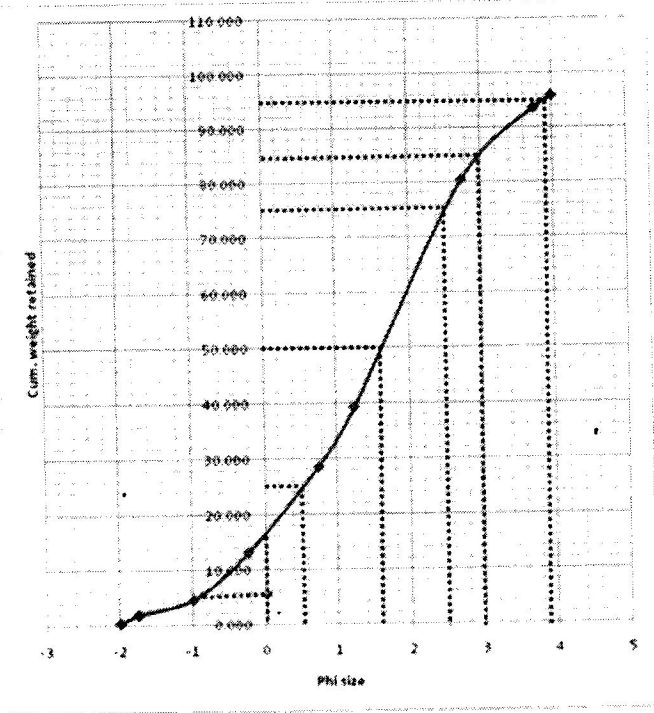


Fig. 4.17: Particle size distribution curve for sample FE3B

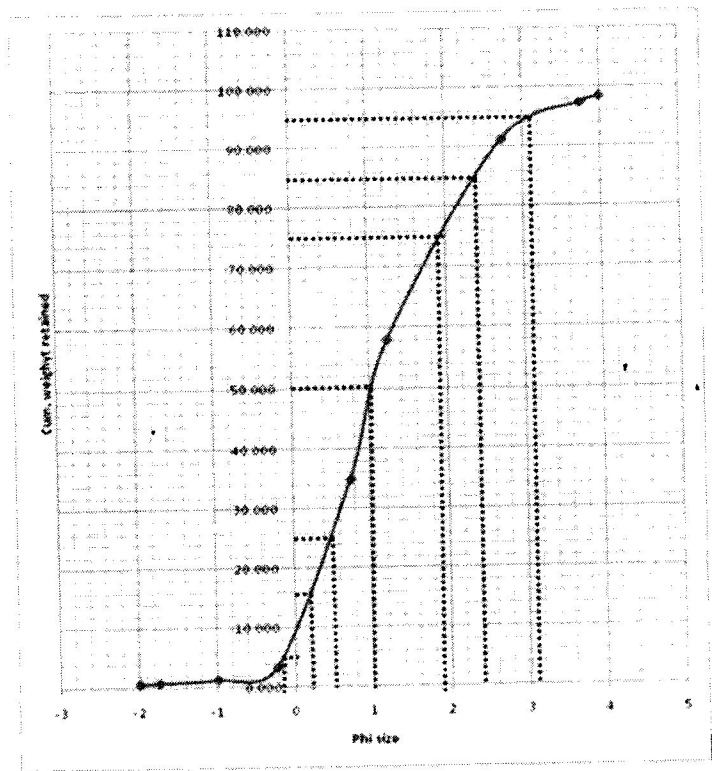


Fig. 4.18: Particle size distribution curve for sample FE3C

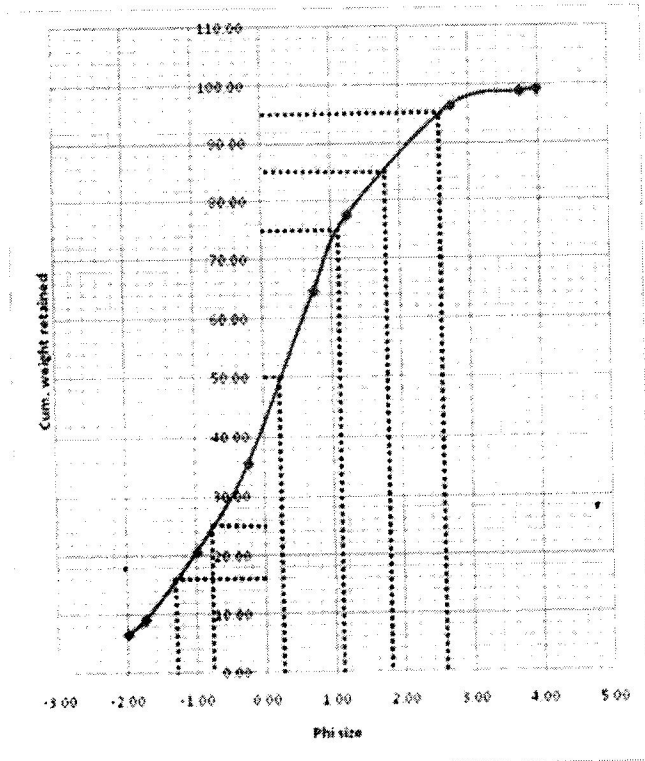


Fig. 4.19: Particle size distribution curve for sample FE3E

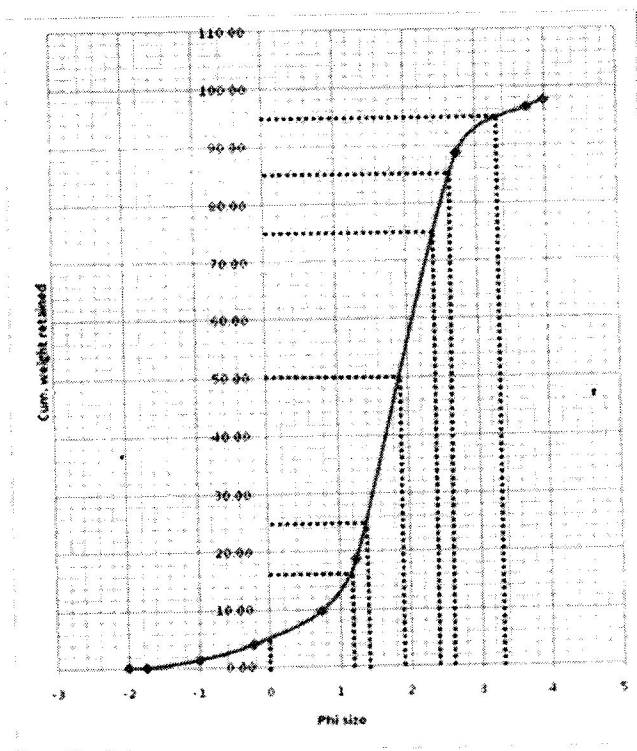


Fig. 4.20: Particle size distribution curve for sample FE3F

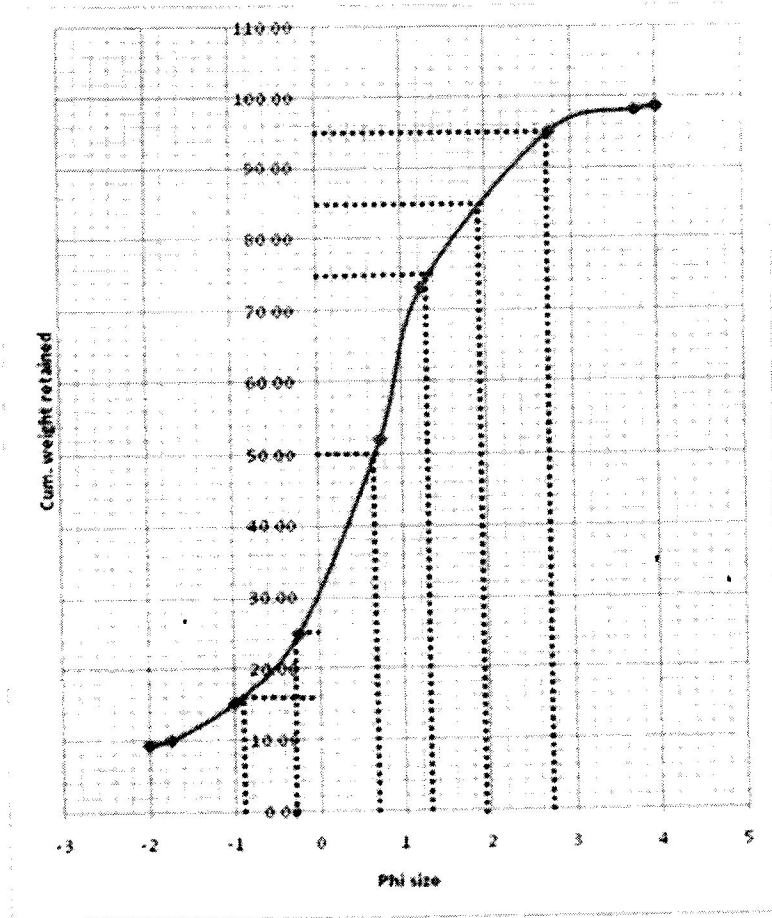


Fig. 4.21: Particle size distribution curve for sample FE3G

TABLE 4.8: Percentile values from Cumulative Curve Plots of Sandstone Samples in the Study Area

SAMPLE NUMBER	$\phi$ 5	$\phi$ 16	$\phi$ 25	$\phi$ 50	$\phi$ 75	$\phi$ 84	$\phi$ 95
FE1B	-0.7	0	0.2	0.8	1.6	2.2	3.25
FE1D	-1.7	-0.9	-0.5	0.2	1	1.8	3.2
FE1E	-3	-1	-0.3	0.4	1.2	1.9	2.7
FE2A	0	0.8	1.1	1.8	2.4	2.8	3.4
FE2B	-0.7	0.3	0.8	1.6	2.4	2.8	3.7
FE2C	-3	-1.4	-0.6	0.5	1.5	2.1	2.9
FE3A	-1	-0.1	0.2	1	1.9	2.4	3.2
FE3B	-0.9	0	0.5	1.6	2.5	3	3.9
FE3C	-0.2	0.2	0.5	1	1.9	2.4	3.1
FE3E	-2.8	-1.3	-1.2	0.1	1.1	1.8	2.6
FE3F	0	1.2	1.4	1.9	2.4	2.6	3.3
FE3G	-	-0.9	-0.3	0.7	1.3	1.9	2.7

The table above shows the percentile values derived from the cumulative graphs drawn with the sieve analysis data. These values were used in the derivation of parameters like the mean, graphic mean, median, inclusive graphic skewness and kurtosis e.t.c.

These are presented in the table below;

Discussions

**Table 4.9:** Table showing Data Interpreted from Calculated Values

SAMPLE NUMBER	GRAPHIC MEAN	INCLUSIVE GRAPHIC STANDARD DEVIATION	INCLUSIVE GRAPHIC SKEWNESS	KURTOSIS
FE1B.	Medium Grained (1)	Poorly sorted (1.14)	Strongly fined skewed (2.54)	Leptokurtic (1.16)
FE1D	Coarse Grained (0.37)	Poorly sorted (1.42)	Strongly fined skewed (3.37)	Leptokurtic (1.34)
FE1E	Coarse Grained (0.43)	Poorly sorted (1.9)	Strongly coarse skewed (-2.99)	Very Leptokurtic (1.56)
FE2A	Medium Grained (1.8)	Poorly sorted (1.01)	Strongly coarse skewed (-0.34)	Mesokurtic (1.07)
FE2B	Medium Grained (1.57)	Poorly sorted (1.23)	Strongly fined skewed (1.68)	Platykurtic (0.77)
FE2C	Coarse Grained (0.4)	Poorly sorted (1.77)	Strongly coarse skewed (-3.77)	Leptokurtic (1.15)
FE3A	Medium Grained (1.6)	Poorly sorted (1.23)	Strongly fined skewed (0.79)	Mesokurtic (1.01)
FE3B	Medium Grained (1.53)	Poorly sorted (1.48)	Strongly coarse skewed (-0.78)	Mesokurtic (0.98)
FE3C	Medium Grained (1.2)	Poorly sorted (1.05)	Strongly fined skewed (2.15)	Mesokurtic (0.97)
FE3E	Coarse Grained (0.2)	Poorly sorted (1.6)	Strongly coarse skewed (-0.62)	Mesokurtic (0.96)
FE3F	Medium Grained (1.9)	Moderately sorted (0.85)	Strongly coarse skewed (-0.83)	Leptokurtic (1.35)
FE3G	Coarse Grained (0.57)	Poorly sorted (1.56)	Strongly coarse skewed (-5.41)	Leptokurtic (1.46)

From the values of the calculated graphic mean in the table above, it can further be inferred that the grain size of the sandstone of the Lokoja Formation ranges from medium grained to coarse grain.

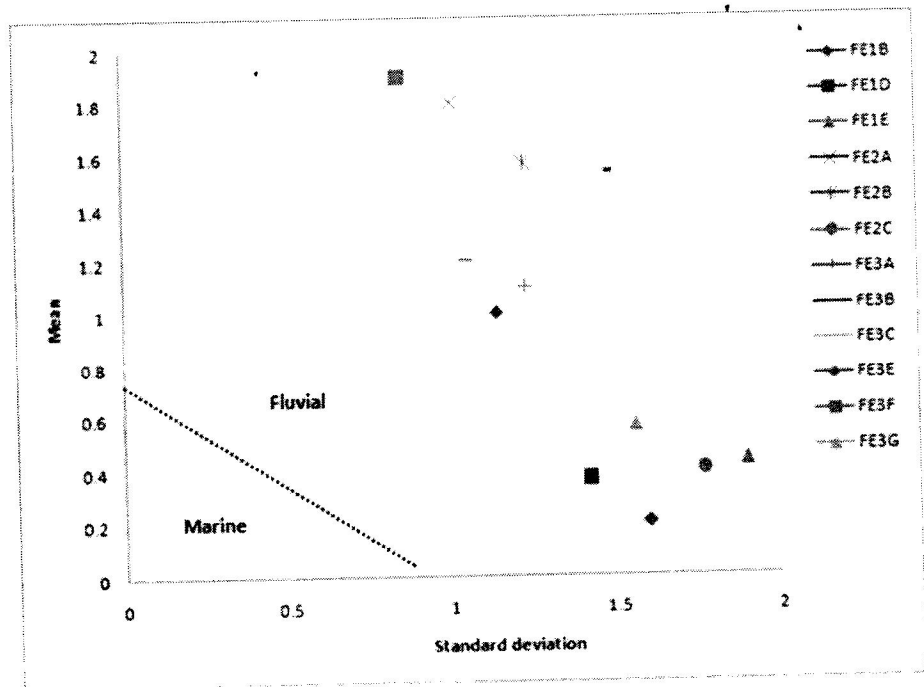


Fig. 4.22: Plots of Mean against Standard deviation (boundary modified after Muiola, R.J., and Wieser D. (1968)).

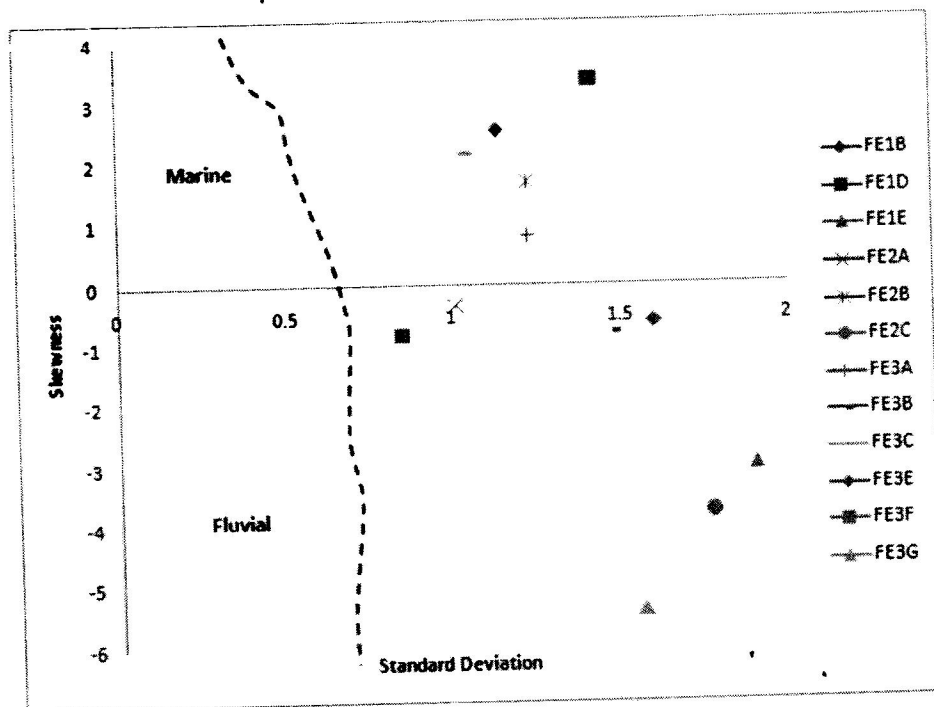


Fig. 4.23: Skewness vs Standard Deviation plots (boundary modified after Muiola, R.J., and Wieser D. (1968))



Sorting values range from 0.55-0.78 as shown in table 9, these values are indicative of poor sorting reminiscent of deposition in a fluvial setting, Friedman G.M., (1967), and thus implying deposition during the regressive out-building of continental facies during the Campanian age in the Middle Niger Basin.

To further establish the fluvial facies defined for the Lokoja Formation using the sorting values in table 4.9, binary plots (Fig. 4.23 and 4.24) with boundaries modified after Moiola, R.J., and Wieser D. (1968) was done for the samples using the skewness, standard deviation and mean values generated from the sedimentological sieve analysis (Table 4.7). Most values plotted falls within the fluvial domains.

### 4.3 Petrography

In order to examine the microtextural and mineralogical features in the thin section of a rock with higher resolution than that of the naked eye, a microscope is used. A microscope has two systems of lenses. The first lens system (objective) produces a magnified image of the object. This real image is viewed by the second lens system (ocular or eyepiece) that also provides further magnification.

4 samples from the study area were selected for thin section petrographic examination, in order to determine their lithology and likely provenance areas. The sandstone have undergone alteration and grain coatings, comprise a range of detrital sandstones, altered igneous grains and sparse metasedimentary rock types. The thin section slides of these samples with their qualitative and quantitative data are presented below (Plate 4.1 - 4.8).

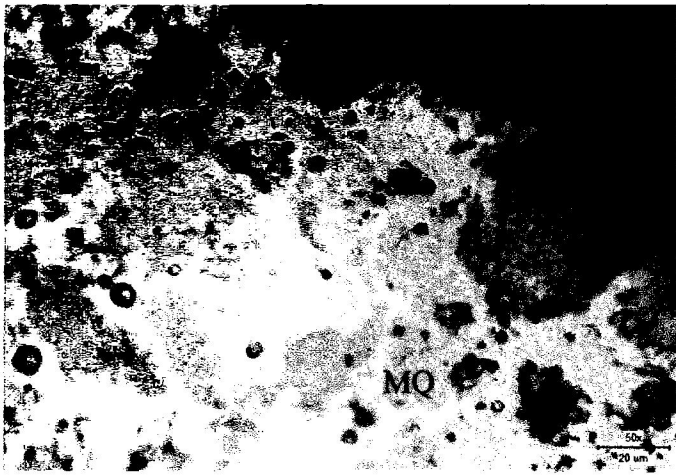


Plate 4.1: Photomicrograph of Lokoja sandstone FE1B under PPL (Mg X50) (MQ - Monocline Quartz, MF - Microcline Feldspar, B- Biotite) (Long.  $07^{\circ} 51' 18''$  E, Lat.  $006^{\circ} 41' 54.5''$  N)

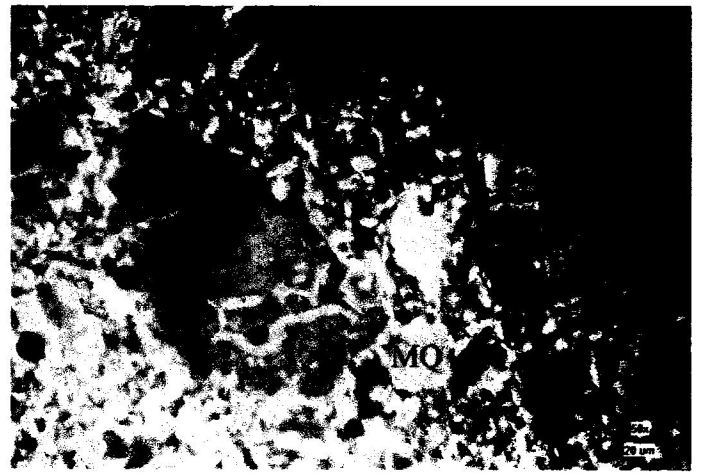


Plate 4.2: Photomicrograph of Lokoja sandstone FE1B under XPL (Mg X50) (MQ - Monocline Quartz, MF - Microcline Feldspar, B- Biotite) (Long.  $07^{\circ} 51' 18''$  E, Lat.  $006^{\circ} 41' 54.5''$  N)

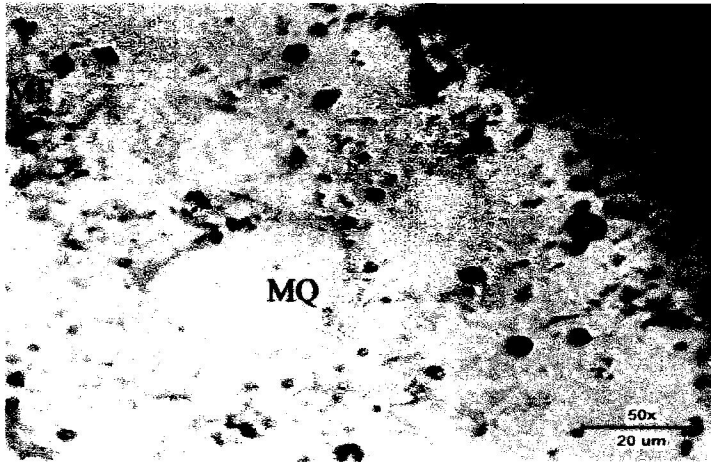


Plate 4.3: Photomicrograph of Lokoja sandstone FE2A under PPL (Mg X50) (MQ - Monocline Quartz, MF - Microcline Feldspar, B- Biotite) (Long.  $06^{\circ} 042' 43''$ , Lat.  $07^{\circ} 51' 15.0''$ )

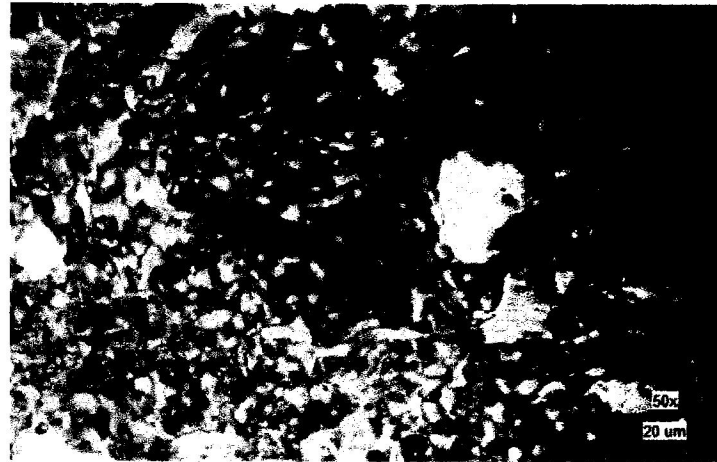


Plate 4.4: Photomicrograph of Lokoja sandstone FE2A under XPL (Mg X50) (MQ - Monocline Quartz, MF - Microcline Feldspar, B- Biotite) (Long.  $06^{\circ} 042' 43''$ , Lat.  $07^{\circ} 51' 15.0''$ )



Plate 4.5: Photomicrograph of Lokoja sandstone FE2D under PPL (Mg X50) (MQ - Monocline Quartz, MF - Microcline Feldspar, B- Biotite) (Long.  $06^{\circ} 042' 43''$ , Lat.  $07^{\circ} 51' 15.0''$ )



Plate 4.6: Photomicrograph of Lokoja sandstone FE2A under XPL (Mg X50) (MQ - Monocline Quartz, MF - Microcline Feldspar, B- Biotite) (Long.  $06^{\circ} 042' 43''$ , Lat.  $07^{\circ} 51' 15.0''$ )

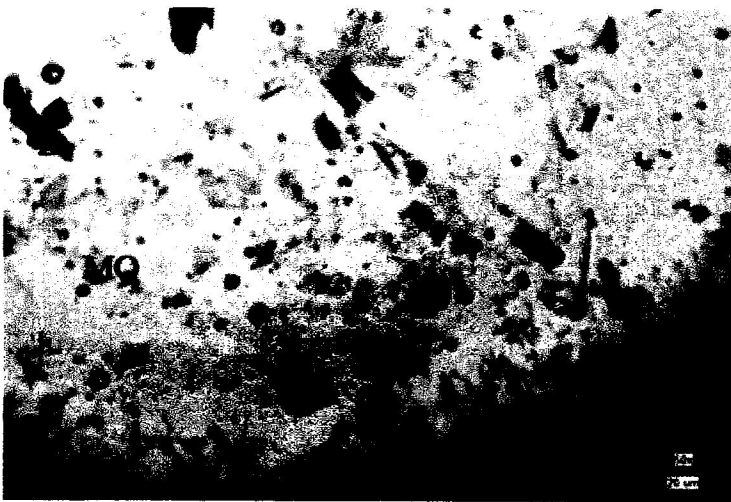


Plate 4.7: Photomicrograph of Lokoja sandstone FE1A under PPL (Mg X50) (MQ - Monocline Quartz, MF - Microcline Feldspar, B- Biotite) (Long.  $07^{\circ} 51' 18''$  E, Lat.  $006^{\circ} 41' 54.5''$  N)

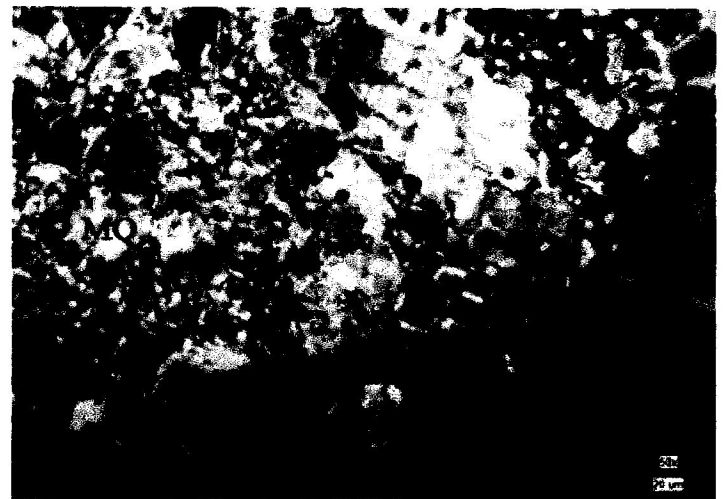


Plate 4.8: Photomicrograph of Lokoja sandstone FE1A under XPL (Mg X50) (MQ - Monocline Quartz, MF - Microcline Feldspar, B- Biotite) (Long.  $07^{\circ} 51' 18''$  E, Lat.  $006^{\circ} 41' 54.5''$  N)

**Table 4.10: Modal Analysis of Sandstone Obtained from Petrography.**

Sample No	Quartz (%)	Feldspar (%)	Rock Fragment (%)	Mineralogical Maturity Index (Q/(F+L) (Nwajide and Hoque, 1985).
FE1A	55	15	5	2.75
FE1B	70	10	10	4.0
FE2A	65	15	10	2.8
FE2D	65	15	20	1.86
AVERAGE	63.75	13.75	11.25	2.7

**Table 4.11: Maturity scale of Sandstone (Nwajide and Hoque, 1985).**

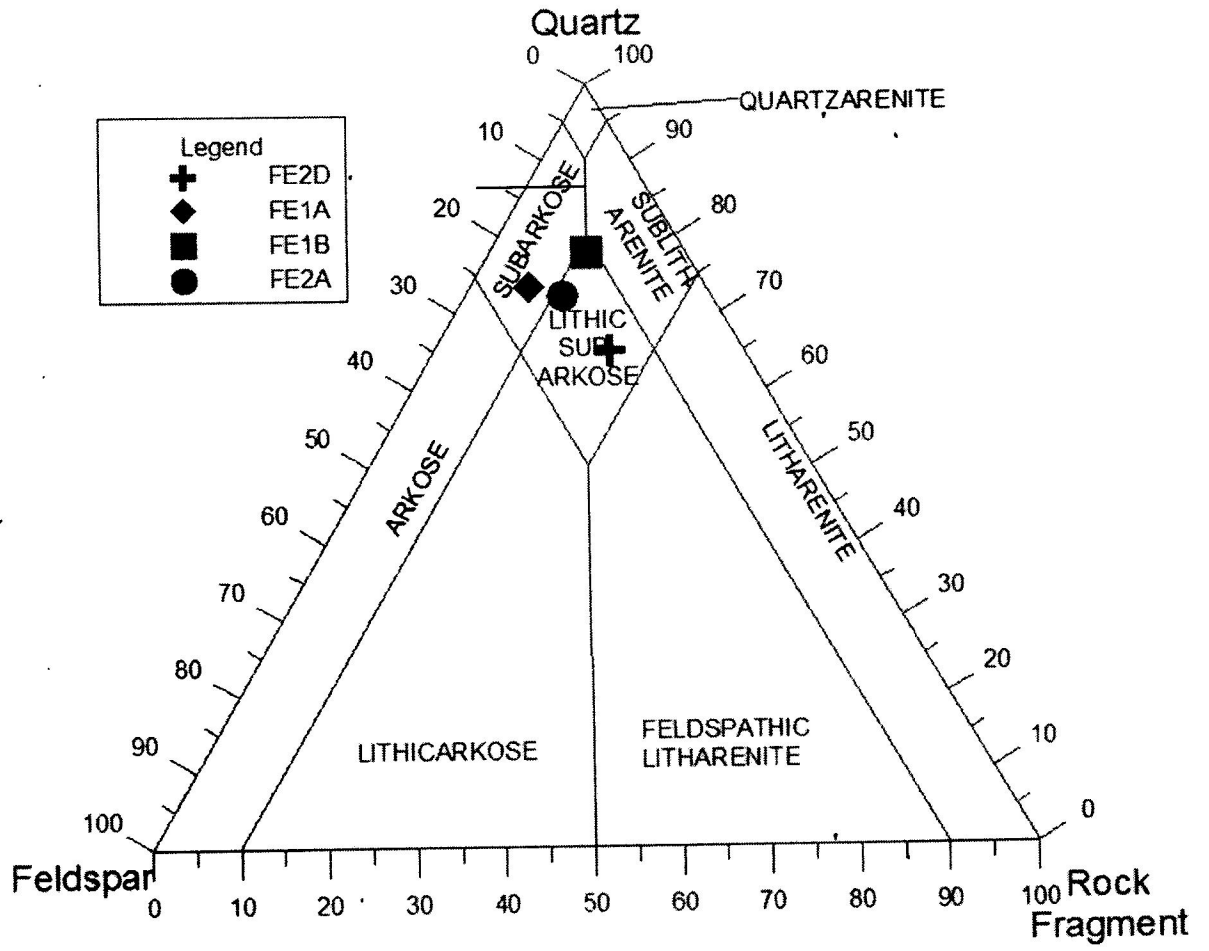
Q $\geq$ 95% (F + RF) = 50%	MI $\geq$ 19 super mature
Q = 95-90% (F + RF) = 5-10%	MI = 19 - 9.0 sub mature
Q = 90-75% (F + RF) = 10-25%	MI = 9.0-3.0 sub mature
Q = 75-50% (F + RF) = 25-50%	MI = 3.0-1.0 immature
Q = < 50	MI $\leq$ 1
(F + RF) > 50%	Extremely immature

(Q - Quartz, F- Feldspar), RF = Rock, F = Fragment, M = Maturity, I= Index

**Maturity:** maturity of the sediment was determined using the (MMI). The mineralogical maturity index is calculated thus;

$$MMI = (\text{Proportion of Qtz}) / (\text{Proportion of Fsp} + \text{Proportion of R.F})$$

Since MMI value is less than 3.0 but greater than 1.0 as calculated above; hence the studied samples are said to be mineralogically immature sediments (Nwajide and Hoque, 1985)



**Figure 4.24:** QFL Ternary Plot of Sandstone in the Study Area (this shows the sandstone to be Arenitic and sub arkose) (After Folks 1974).

#### 4.4 Heavy Mineral Analysis

Heavy mineral analysis was carried out on seven samples from the Filele study area which were suspended into both Xpl and Ppl slides to be viewed under the microscope for further analysis.

From the heavy mineral photomicrograph, it was observed the dominant accessory heavy minerals are composed mainly of opaque minerals; magnetite and ilmenite are good examples of opaque minerals. Two main mineral groups: the opaque and nonopaque were observed in the sandstone samples of Filele as indicated in the photomicrograph below. The non-opaque minerals include zircon, tourmaline, rutile, staurolite, epidote, sillimanite, apatite and garnet. Such heavy minerals assemblages are typical of igneous and metamorphic provenance of the nearby basement complex. Zircon is present in significant amount as dominant non opaque, ultra-stable mineral. Zircon is recognized in thin section by its high relief, colourless appearance, prismatic habit as well as its very high interference colours. It forms about 20% of the heavy mineral suite in all the sandstones. Tourmaline is identified by its high relief, pleochroic nature and absence of cleavage with good prismatic habit. The results indicated the dominance of ultra-stable heavy minerals over the metastable and unstable varieties. Rutile occurs as small, reddish-brown prismatic to acicular crystals with very high relief and high interference colours. The zircon, tourmaline, and rutile (ZTR) index of mineralogical modification (Hubert, 1962) was calculated for the analyzed samples (Table 4.12) by finding the ratio of the combined proportion of zircon, tourmaline and rutile to the total weight of all the transparent heavy minerals present.

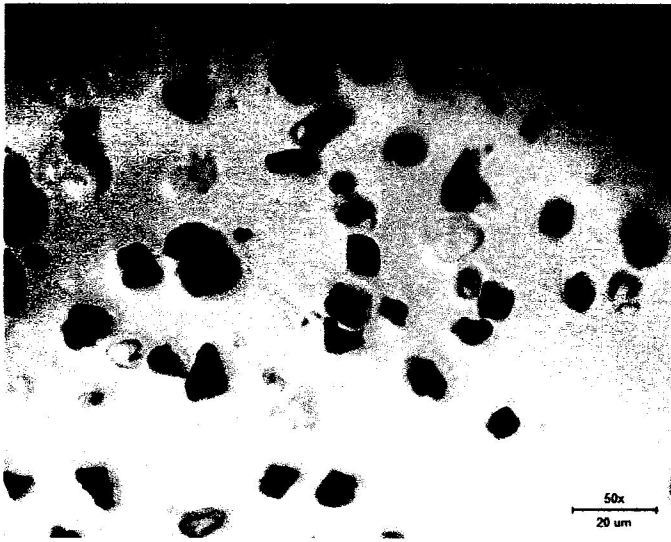


Plate 4.9: Photomicrograph of heavy minerals in Lokoja sandstone (FE1B) showing Zircon (Z), Opaque Minerals (Op), Tourmaline (Tr), Rutile (R) under PPL (Long.  $07^{\circ} 51' 18''$  E, Lat.  $006^{\circ} 41' 54.5''$  N)

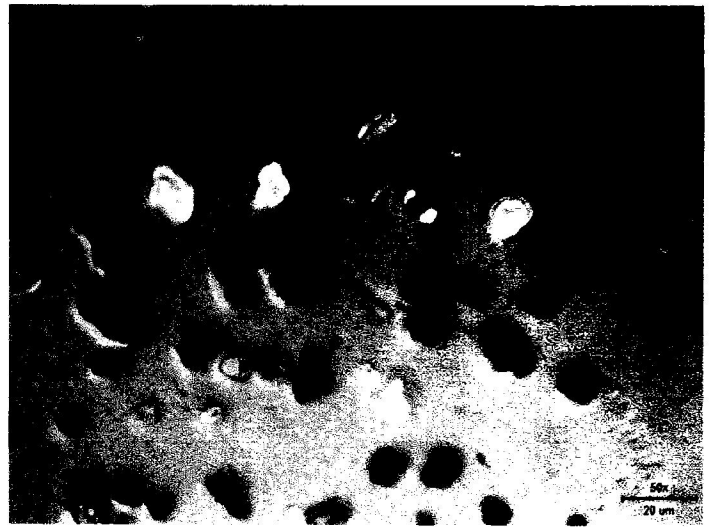


Plate 4.10: Photomicrograph of heavy minerals in Lokoja sandstone (FE1B) showing Zircon (Z), Opaque Minerals (Op), Tourmaline (Tr), Rutile (R) under XPL (Long.  $07^{\circ} 51' 18''$  E, Lat.  $006^{\circ} 41' 54.5''$  N)



Plate 4.11: Photomicrograph of heavy minerals in Lokoja sandstone (FE1C) showing Zircon (Z), Opaque Minerals (Op), Tourmaline (Tr), Rutile (R) under PPL (Long.  $07^{\circ} 51' 18''$  E, Lat.  $006^{\circ} 41' 54.5''$  N)



Plate 4.12: Photomicrograph of heavy minerals in Lokoja sandstone (FE1C) showing Zircon (Z), Opaque Minerals (Op), Tourmaline (Tr), Rutile (R) under XPL (Long.  $07^{\circ} 51' 18''$  E, Lat.  $006^{\circ} 41' 54.5''$  N)

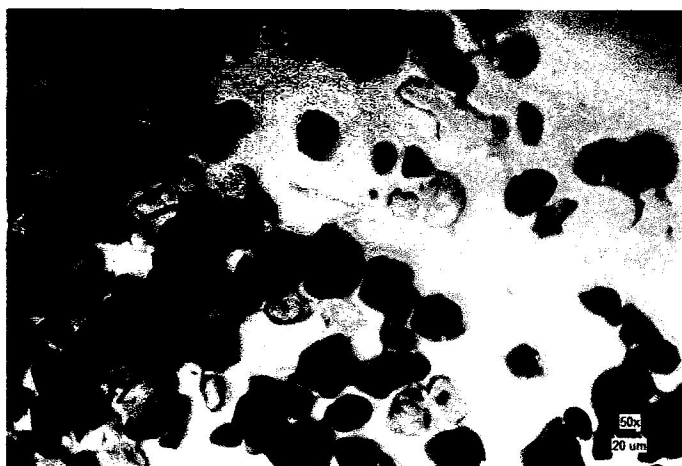


Plate 4.13: Photomicrograph of heavy minerals in Lokoja sandstone (FE2B) showing Zircon (Z), Opaque Minerals (Op), Tourmaline (Tr), Rutile (R) under PPL (Long.  $06^{\circ} 042' 43''$ , Lat.  $07^{\circ} 51' 15.0''$ )



Plate 4.14: Photomicrograph of heavy minerals in Lokoja sandstone (FE2B) showing Zircon (Z), Opaque Minerals (Op), Tourmaline (Tr), Rutile (R) under XPL (Long.  $06^{\circ} 042' 43''$ , Lat.  $07^{\circ} 51' 15.0''$ )

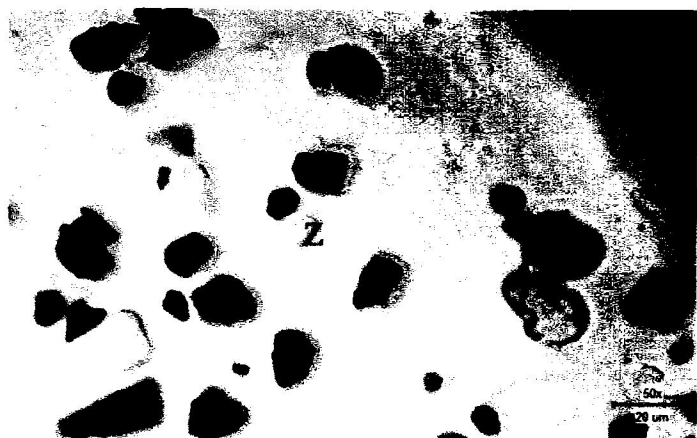


Plate 4.15: Photomicrograph of heavy minerals in Lokoja sandstone (FE3C) showing Zircon (Z), Opaque Minerals (Op), under PPL (Lat.  $07^{\circ} 51' 11''$ N, Long.  $06^{\circ} 42' 59''$ E)

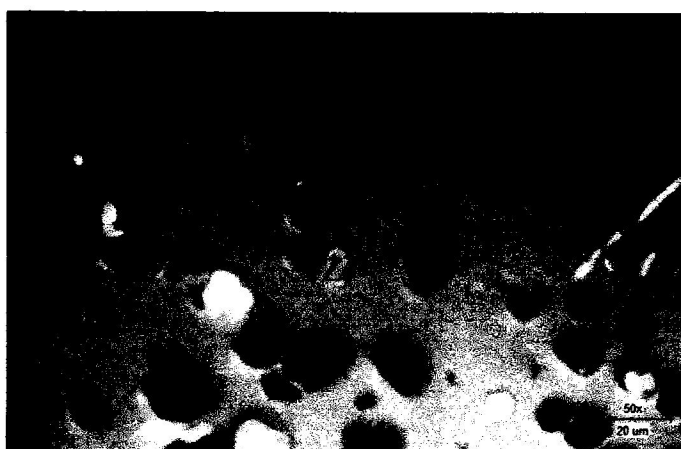


Plate 4.16: Photomicrograph of heavy minerals in Lokoja sandstone (FE3C) showing Zircon (Z), Opaque Minerals (Op), under XPL (Lat.  $07^{\circ} 51' 11''$ N, Long.  $06^{\circ} 42' 59''$ E)



**Table 4.12: Percentage Composition of the Non-opaque and Opaque Heavy Mineral Suites in the Study Area**

SAMPLE NO	Z (%)	Tr (%)	R (%)	Op (%)	Non Op (%)	ZTR Index (Hubbert, 1962)
FE1B	15	4	8	60	40	53
FE1C	20	5	10	50	50	65
FE2B	18	4	9	55	45	59
FE3C	25	5	10	50	50	60

**Key:** Z - Zircon, Tr – Tourmaline, R – Rutile, Op – Opaque minerals, Non Op – Non Opaque Minerals, ZTR index – Zircon, Tourmaline, Rutile index.

The ZTR index (Hubbert, 1962) ranges from 53 – 65% (Table 4.12) which indicates immature sandstone derived from the nearby granite and gniesses probably the western basement complex around Lokoja.

#### 4.5 Geochemistry

Five samples were subjected to geochemical analysis. Four out of those five are conglomeratic sandstone, while one is Gneiss.

##### Major Elements Geochemistry

The results of the major oxides are shown in Table 5. The elemental oxides of the Lokoja Sandstone are; 63.4-67% SiO<sub>2</sub>; 13.43-13.48% Al<sub>2</sub>O<sub>3</sub>; 2.14-3.23% Fe<sub>2</sub>O<sub>3</sub> ; 0.59-3.06% CaO; 3.34-4.28% Na<sub>2</sub>O; 2.09-2.93% K<sub>2</sub>O and 0.57-1.09% TiO<sub>2</sub>. Other oxides such as NiO and CuO are less than 1%. The Fe<sub>2</sub>O<sub>3</sub> value is relatively low (< 4%) in the three conglomeratic sandstone samples while that of the weathered basement is the highest 7.67%.

Titanium is mainly concentrated in phyllosilicates and is relatively immobile compared to other elements during various sedimentary processes and may strongly represent the source rocks (McLennan et al., 1993), the titanium oxides for all samples are relatively low with values less than 2%.

The low concentrations of Fe<sub>2</sub>O<sub>3</sub> + TiO + MgO imply that the sediments are chemically inert and non-corrosive. The values of the silica-alumina ratios for the samples strongly support that it is highly siliceous.

Cross plots of % SiO<sub>2</sub> versus Fe<sub>2</sub>O<sub>3</sub>; SiO<sub>2</sub> versus Al<sub>2</sub>O<sub>3</sub> and SiO<sub>2</sub> versus LOI (Fig. 4.26) all indicate negative correlation. These demonstrate influence of weathering processes through enrichment of silica and depletion of Fe and Mg as well as the decrease in LOI with increasing weathering and maturity of the sediments. The negative correlation between SiO<sub>2</sub> and Al<sub>2</sub>O<sub>3</sub> is also an indication of the fact that most of the silica is present as quartz grains (Tijani et al., 2010). However, the positive correlation between Fe<sub>2</sub>O<sub>3</sub> and Al<sub>2</sub>O<sub>3</sub> is an indication of a common source. Positive correlations with Al<sub>2</sub>O<sub>3</sub> are shown by most of the major elements. It can be concluded, therefore, that the enrichment of other major elements in the Lokoja Sediments is related to the enrichment of ferromagnesian minerals and feldspars probably due to short transportation of the source materials.

**Table 4.13:** Table showing Major oxides and their percentage.

Oxide Composition (%)	FE1D	FE2C	FE3E	FE1A	FE1C
SiO <sub>2</sub>	65.26	69.29	63.4	52.37	67
TiO <sub>2</sub>	1.09	0.58	0.57	1.62	0.91
Al <sub>2</sub> O <sub>3</sub>	13.43	13.44	13.48	15.89	13.45
Fe <sub>2</sub> O <sub>3</sub>	2.14	3.23	2.25	7.67	2.52
CaO	1.74	0.59	3.06	6.06	1.33
MgO	0.7	0.22	1.1	3.11	0.67
Na <sub>2</sub> O	4.28	3.34	3.94	4.04	3.49
K <sub>2</sub> O	2.7	2.09	2.31	2.1	2.93
MnO	0.086	<0.001	<0.001	0.078	<0.001
V <sub>2</sub> O <sub>5</sub>	0.03	0.039	0.01	0.04	0.03
Cr <sub>2</sub> O <sub>3</sub>	0.09	0.084	0.069	<0.001	0.069
CuO	0.07	0.045	0.051	0.09	0.067
NiO	0.006	ND	ND	ND	ND
As <sub>2</sub> O <sub>3</sub>	0.009	0.01	0.017	0.004	0.01
ZrO <sub>2</sub>	0.15	0.054	0.06	0.21	0.18
BaO	0.36	0.19	0.26	ND	0.2
PbO	0.064	0.02	0.041	0.085	0.05
ZnO	ND	ND	ND	0.024	ND
SrO	0.18	0.11	0.231	0.24	0.17
Rb <sub>2</sub> O	0.091	0.044	0.065	0.14	0.087
Ga <sub>2</sub> O <sub>3</sub>	0.02	0.015	ND	0.02	0.005
Cl	ND	ND	ND	ND	ND
L.O.I	7.5	6.6	9.1	6.2	6.9
Total	99.99	99.99	100	99.99	100
SiO <sub>2</sub> /Al <sub>2</sub> O <sub>3</sub>	4.85927	5.156	4.70326	3.29578	4.98141
K <sub>2</sub> O/Na <sub>2</sub> O	0.63084	0.626	0.58629	0.5198	0.83954
Al <sub>2</sub> O <sub>3</sub> /TiO <sub>2</sub>	12.3211	23.17	23.6491	9.80864	14.7802
Log(K <sub>2</sub> O/Na <sub>2</sub> O)	0.20008	-0.204	-0.2319	-0.2842	-0.076
CIA	60.6321	69.06	59.1487	56.5682	63.4434
Log(Fe <sub>2</sub> O <sub>3</sub> /K <sub>2</sub> O)	-0.10095	0.189056236	-0.0114	0.56258	-0.0655
Log(SiO <sub>2</sub> /Al <sub>2</sub> O <sub>3</sub> )	0.686571	0.712312909	0.6724	0.51796	0.69735
Discriminant function 1	-2.3486	-0.3301	-0.7951	-	-2.6197
Discriminant function 2	3.5453	4.5163	3.6247	-	5.3576

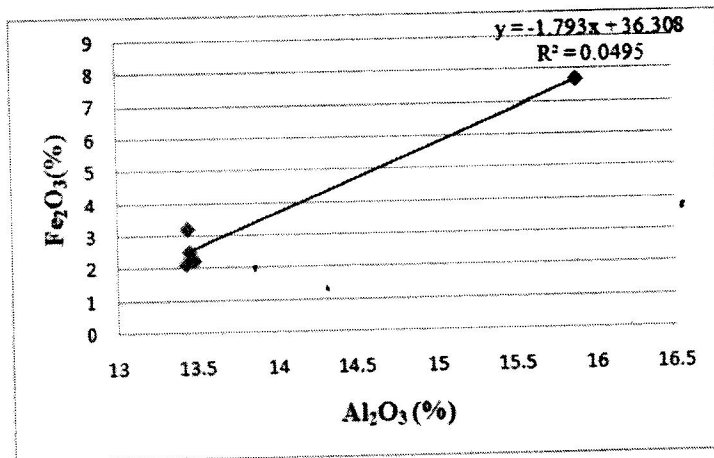
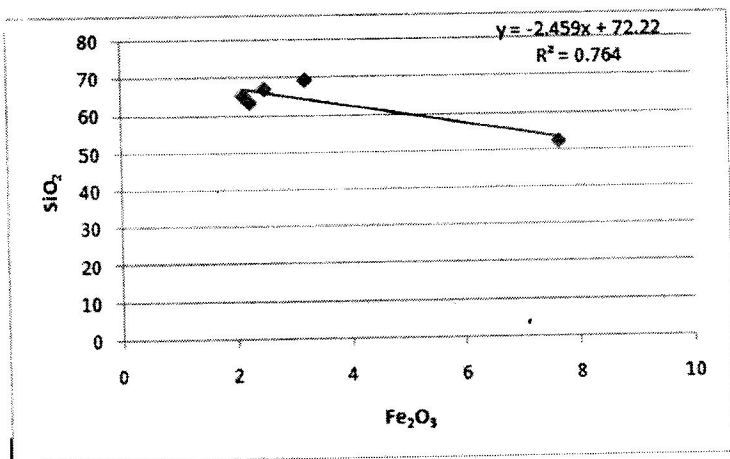
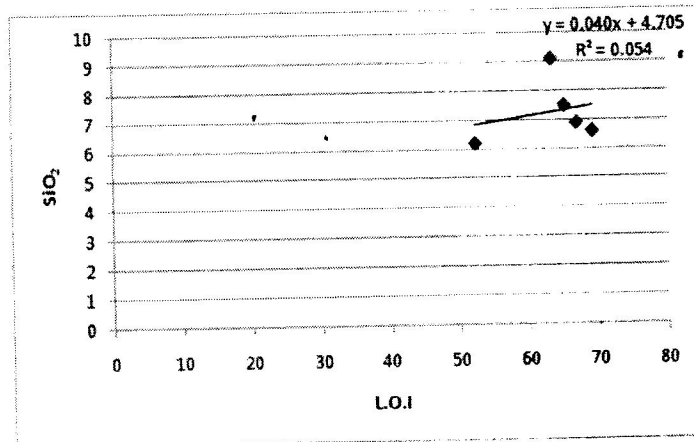
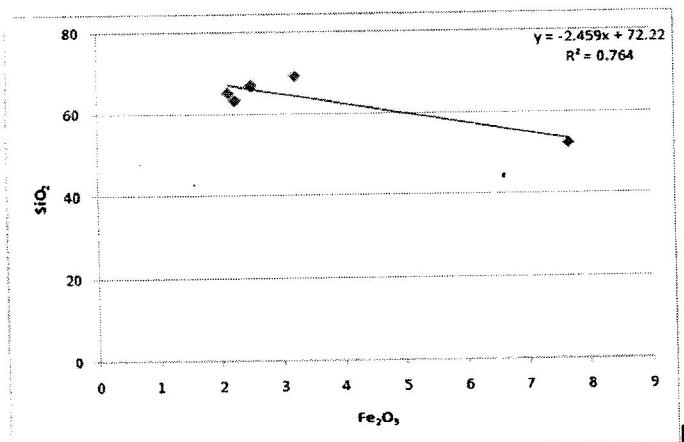


Fig. 4.25: Cross Plots of Major Oxides:  $\text{SiO}_2$  against  $\text{Fe}_2\text{O}_3$ ,  $\text{SiO}_2$  against  $\text{Al}_2\text{O}_3$ ,  $\text{SiO}_2$  against L.O.I,  $\text{Fe}_2\text{O}_3$  against  $\text{Al}_2\text{O}_3$ .

## 4.6 Provenance

### Geochemical Provenance

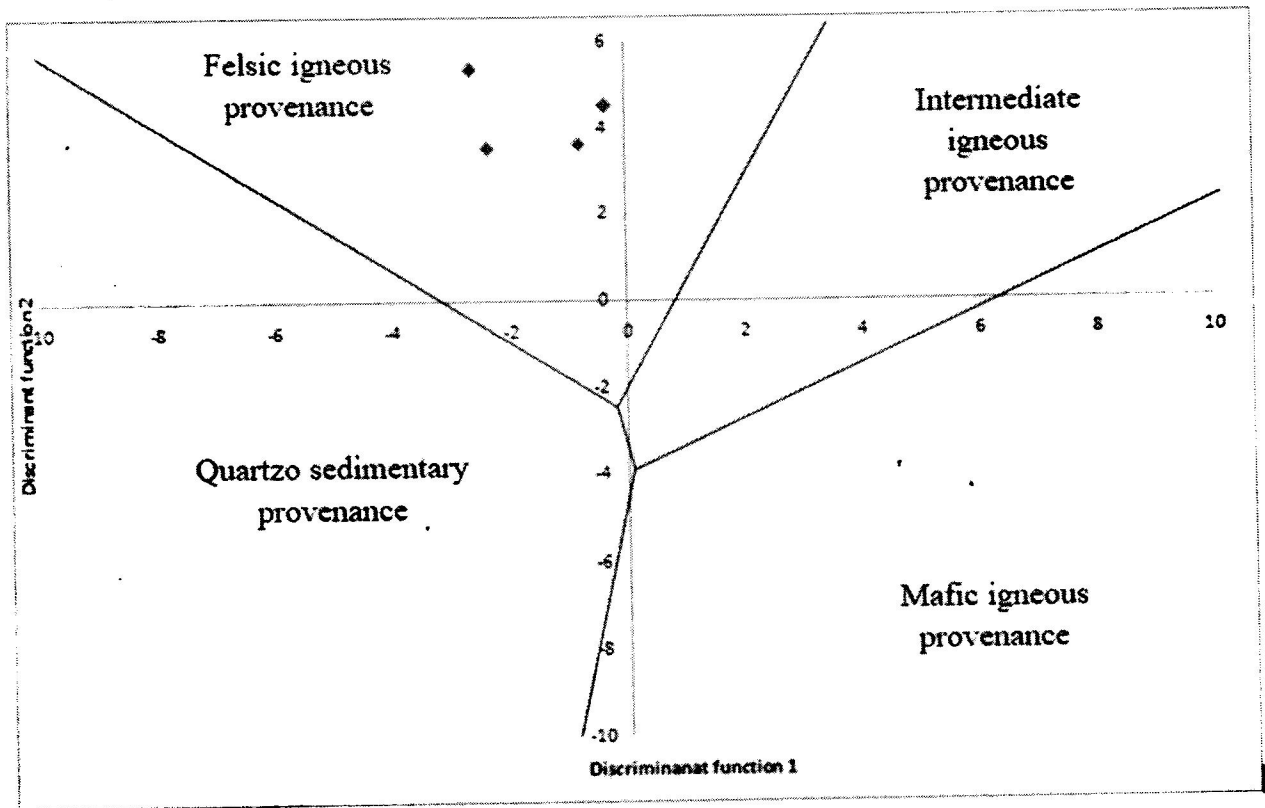
Several classifications have been proposed to discriminate from various tectonic settings (Maynard et al., 1982; Bhatia, 1983; Bhatia and Crook, 1986; Roser and Korsch, 1986). The provenance signature study employed for this study helps distinguish the sources of the sediments into four provenance zones, mafic, intermediate or felsic, igneous and quartzose sedimentary. This discriminant function diagram proposed by Roser and Korsch (1986) makes use of the oxides of Ti, Al, Fe, Mg, Ca, Na and K to effectively differentiate the sediments into four provenance zones. They also noted that biogenic CaO and SiO<sub>2</sub> in provenance determination could be eliminated by a plot in which the discriminant functions are based upon the ratios of TiO<sub>2</sub>, Fe<sub>2</sub>O<sub>3</sub>, MgO and K<sub>2</sub>O all to Al<sub>2</sub>O<sub>3</sub> though it is not as effective as the one based upon the raw oxides. The discriminant functions for the two plots used to discriminate the sediments from the study area are as follows:

The formula for raw oxides is given as:

$$\text{Discriminant Function (DF1)} = -1.773\text{TiO}_2 + 0.607\text{Al}_2\text{O}_3 + 0.76\text{Fe}_2\text{O}_3 (\text{T}) - 1.5\text{MgO} + 0.616\text{CaO} + 0.509\text{Na}_2\text{O} - 1.224\text{K}_2\text{O} - 9.09$$

$$\text{Discriminant Function (DF2)} = 0.445\text{TiO}_2 + 0.07\text{Al}_2\text{O}_3 - 0.25\text{Fe}_2\text{O}_3 (\text{T}) - 1.42\text{MgO} + 0.438\text{CaO} + 1.475\text{Na}_2\text{O} + 1.426\text{K}_2\text{O} - 6.861.$$

From the discriminant function diagram shown below, it can be said that the sandstone of the Lokoja formation is of Igneous provenance.



**Fig. 4.26:** Discriminant Function diagram for provenance signature for Lokoja formation sediments using raw oxide (after Roser and Korch 1988)

### **Heavy mineral provenance**

The heavy mineral assemblages from the sandstones of the studied area show an abundance of both non-opaque and opaque minerals. The heavy minerals of this type of assemblage were derived mostly from igneous and metamorphic rocks.

According to Heinrich (1956) the presence of tourmaline and epidote is suggestive of low to medium grade metamorphic provenance. The zircon grains in sandstones are diverse types and regarded as the best provenance indicator and one of the most resistant minerals among all the heavy minerals (Pettijohn, 1975).

The colourless sub-angular to sub-rounded zircon grains indicate their derivation from igneous source rocks (Pettijohn, 1975). Tourmaline occurring as prismatic grains with green bluish type and brown colour indicate granite and pegmatite derivation (Krynine, 1946). A sub-rounded form of tourmaline indicates a short transportation. Opaque minerals indicate chemical leaching of the sediments. Opaque minerals are mainly derived from crystalline igneous rocks both acidic and basic. Presence of green tourmaline grains favour their derivation from igneous sources, Colourless, sub-angular to sub-rounded grains of zircon indicate its derivation from igneous source. Zircon, rutile and tourmaline show an acid igneous source. Higher proportion of opaque mineral indicates an igneous source. The Heavy minerals present in the sandstone samples suggests an igneous provenance for the Lokoja sandstone.

#### 4.7 Paleoenvironments

The paleodepositional environment strongly indicated by various environmental diagnostic parameters obtained from pebble morphometry data is fluvial (Table 4.5). Roundness is a poor indicator of depositional environment, Sneed and Folk (1958) observed that pebble roundness increased downstream from river to beaches, roundness of less than 35% typifies fluvial environment while roundness of more than 45% characterizes littoral environments. The average roundness value of the pebbles from the study area is  $35.73\% \pm 7.137$  and 60% of the pebble having roundness varying from 20 – 45%. This result very much implies a fluvial depositional environment. This is further corroborated by Sames' (1966) plot of roundness versus elongation (I/L) which shows 60% of the pebbles in the fluvial field while 10% lie in the littoral field. The pebbles under investigation fall within the fluvial field using the bivariate plot of sphericity against oblate – prolate index (Dobkins and Folk, 1970).

Plots of mean against standard deviation also support the fluvial origin for these sediments (Fig. 4.22), it can be seen that all the samples fall in the fluvial boundary of the plot. (Moiola, R.J., and Wieser D. (1968)). All these agree that the Lokoja Formation is of Fluvial origin.



## Chapter Five

### Conclusions

#### 5.1 Conclusions

The pebble morphometric parameters have shown a strong indicator for distinguishing paleodepositional environment, a few sedimentary structures also indicate a shallow marine environment. The subsequent parameters obtained in the pebble morphometric analysis together, with bivariate plots have shown that the depositional environment of the basal Lokoja Formation is principally swayed by fluvial processes with few beach/ littoral influence.

One main lithofacies, sand, and two sub-lithofacies (medium-grained sand, coarse-grained sand) were defined. Sorting ranged from 0.85 – 1.56, indicating poor – moderate sorting for the Lokoja Formation. Depositional environments defined by values of binary plots of skewness versus standard deviation mean versus standard deviation for samples obtained from the Lokoja area, indicate that sediments of the Lokoja Formation was deposited in a continental fluvial paleodepositional environment.

From the geochemical data Positive correlations with  $Al_2O_3$  are shown by most of the major elements. It can be concluded, therefore, that the enrichment of other major elements in the Lokoja Sediments is related to the enrichment of ferromagnesian minerals and feldspars probably due to short transportation of the source materials. From our heavy mineral analysis the results indicated the dominance of ultra-stable heavy minerals over the metastable and unstable varieties.

From the petrographic data studied, the Lokoja sandstone is mineralogically immature and its provenance is not far from the basin in which it was deposited.

## References

- Abimbola, A.F. 1997. Petrographic and paragenetic studies of the Agbaja Ironstone Formation, Nupe Basin, Nigeria. *Journal of African Earth Sciences* 25, 169-181
- Abimbola, A.F., Badejoko, T.A; Elueze, A.A., and Akande, S.O. 1999. The Agbaja Ironstone Formation, Nupe Basin, Nigeria. A product of replacement of a Kaolinite precursor. *Global Journal of Pure and Applied Sciences* 5: 375-384
- Adeleye, D.R. 1973. Origin of ironstones, an example from the Middle Niger valley, Nigeria. *Journal of Sedimentary Petrology* 43: 709-727
- Adeleye, D.R., (1972). Sedimentology of the fluvial Bida Sandstones (Cretaceous) Nigeria. *Sedimentary Geology* 12:1-24.
- Adeleye, D.R., The Geology of the middle Niger Basin, In, Kogbe, C.A.(Ed), *Geology of Nigeria, 2nd Rock view (Nigeria) Ltd, Jos, p.335-339.*
- Agyingi, C.M. 1991. Geology of Upper Cretaceous rocks in the eastern Bida Basin, Central Nigeria. *Unpublished Ph.D. Thesis, University of Ibadan, Nigeria, 501pp.*
- Akande SO, Erdtmann BD (1998) Burial metamorphism (thermal maturation) in Cretaceous sediments of the Southern Benue Trough and Anambra Basin, Nigeria. *AAPG Bull* 82: 1191-1206.
- Akande, S.O., Ojo, O.J. and Ladipo, K.O. 2005. Upper Cretaceous Sequence in the Southern Bida Basin, Nigeria: A Field Guide book. NAPE Geological Field Guid No. 1. Mosuro Publishers, Ibadan, 60p.
- Benkhelil J (1989) The origin and evolution of the Cretaceous Benue Trough, Nigeria. *J Afr Earth Sci* 8:251-282
- Bhatia M. R., 1983. Plate tectonics and geochemical composition of sandstones, *J. Geol.* 91, 611 - 627.
- Bhatia M. R., Crook A. W., 1986. Trace element characteristics of graywackes and tectonic setting discrimination of sedimentary basins, *J. Geol.* 92, 181 - 193.
- Braide, S. P. (1992). Geological development, origin and energy mineral resources potential of the Lokoja Formation in the southern Bida Basin. *Journal of Mining and Geology*, 28, 33-44.

- Dickinson W.R. 1988. Provenance and sediment dispersal in relation to paleotectonics and paleogeography of sedimentary basin. In: Kleinspehn, K.L, Paola, C. (Eds), *New perspectives in Basin Analysis*. Springer – Verlag, New York, pp 3 – 25
- Dickinson, W. R. 1970. Interpreting detrital model of greywacke and arkose. *Journal of Sedimentary Petrology*, 40, 695 – 707
- Dickinson, W. R. and Suczek, C. A. 1979. Paleotectonic and sandstone compositions. *Bull. American Association of Petroleum Geologists*, 63, 2164-2182
- Dickinson, W.R. 1985. Interpreting provenance relations from detrital models of sandstones. In: Zuffa, G.G (Eds), *Provenance of Arenites*. Reidel Pub. Dordrecht. Pp 333 – 361
- Dobkins, J. E. and Folk, R. L. 1970. Shape development on Tahiti – Nui. *Journal of Sedimentary Petrology*, 40, 1167-1203
- Dobkins, J.E. and Folk, R.L. 1970. Shape development of Tahiti- Nui: *Journal of Sedimentary Petrology*, 40, pp. 1167 – 1203.
- Falconer, J.D. 1911. *The Geology and Geography of Northern Nigeria*, Macmillan, London 255pp
- Folk, R. L. 1974. *Petrology of sedimentary rocks*. Hemphil, Austin, Texas, 182p.
- Folk, R.L., Ward, W. (1957). Brazos Riverbar. A study in the significance of grain size parameter. *Journal of sedimentary Petrology*, 27, 3-26.
- Friedman G.M., (1967), Dynamic processes and statistical parameters compared for size frequency distribution of beach and river sands, *J. Sediment. Petrol.*, 37, 327–354.
- Heinrich, E.W., 1956. *Microscopic petrography*. McGraw Hills, New York, 418p.
- Hubbert, J.F. 1962. *A zircon-tourmaline-rutile maturity index and interdependence of the composition of heavy mineral assemblages with the gross composition and texture of rocks*. *Journ. Sed. Petrology* Vol. 32 pp 440-450.
- Hubert., F.L.1968. Selection and wear of pebbles on Gravel Beach, University of Groningen, Geological Institute Publication. P. 144
- Idowu, J. O., & Enu, E. I. (1992). Petroleum geochemistry of some late Cretaceous shale from the Lokoja Sandstone of Middle Niger Basin, Nigeria. *Journal of African Earth Sciences*, 14, 443-455.

- Jan Du Chene, R. E., Klasz, I.D.E., Archibong, E. E. Biostratigraphic study of the borehole Ojo 1, SW Nigeria, with special emphasis on the Cretaceous Microfloral. *Revue de Micropaleontology*, 1979; 21, 123-139
- Jones, H. A. 1953. The occurrence of oolitic ironstone in Nigeria: their origin, geological history and petrology. D. Phill thesis, Oxford University, 244pp
- Jones, H.A. 1958. The oolitic Ironstone of Agbaja Plateau, Kabba province. *Records of Geol. Survey of Nigeria*, 1955.p. 20-43
- Krynine, P.D., 1946. The tourmaline group in sediments. *Jour. Geol.*, Vol.54, pp.65-87.
- Ladipo, K.O., Akande, S.O., Mucke, A. 1994. Genesis of ironstones from middle Niger Sedimentary basin, evidence from sedimentological, ore microscope and geochemical studies. *Journal of Mining and Geology* 30, 161-168
- Ladipo, K.O., Ojo, O.J. and Akande, S.O. 2011. Field trip guide to the Upper Cretaceous sequences of the southern Bida Basin: An overview of the petroleum system. *Publication of the Nigerian Association of Petroleum Explorationists* 22p
- Ladipo, K.O., Nwajide, C.S., Akande, S.O., and Mucke, A., 1994. Genesis of oolitic Ironstone from Middle Niger Sedimentary Basin: evidence from sedimentological, Ore microscopic and geochemical studies. *J. Mining and Geol.*, V. 30, p. 161-168.
- Lutig, G. 1962. The shape of pebbles in the continental fluvial and marine facies. *Int. Assoc. Scientific Hydrology Pub.* 59, 235 -258
- Maynard J. B., Valloni R. and Ho Shing Ju, 1982. Composition of modern deep-sea sands from arc-related basin. *J. Geol. Soc. Am. Spec. Publs.*, No. 10, 551 - 561.
- McLennan, S. M., Hemming, S., McDaniel, D. K., & Hanson, G. N. (1993). Geochemical approaches to sedimentation, provenance, and tectonics. *Special Papers-Geological Society of America*, 21-21. <http://dx.doi.org/10.1130/SPE284-p21>.
- Moiola, R.J., and Wieser D. (1968). Textural parameters; an evaluation, *Jour. Sed. Petro.*, 38; 45-53
- Nton, M.E. and Okunade, A. 2013. Aspects of hydrocarbon potential and clay mineralogy of the Patti Formation, Southern Bida Basin, Central Nigeria. *Nigeria Association of Petroleum Explorationists Bulletin* Vol 25(1), pp 15 - 28.

- Nwajide, C.S, Hoque, M. (1985). Application of Markov chain and entropy analysts to lithologic successions: an example from the Cretaceous of the Benue trough, Nigeria. *Geolog. Rundschau*, v.74,p 165-177.
- Nwajide, C.S., 2013 *Geology of Nigeria's Sedimentary Basin*. P. 183
- Obaje, N. G., Balogun D. O., Idris-Nda A., Goro I. A., Ibrahim S. I., Musa M. K., Dantata S. H., Yusuf I., Mamud-Dadi N. and Kolo I. A. 2013. Preliminary Integrated Hydrocarbon Prospectivity Evaluation of the Bida Basin in North Central Nigeria. *Petroleum Technology Development Journal*, 3 (2): 36 – 65.
- Obaje, N. G., Wehner, H. and Scheeder, G. 2004. Hydrocarbon prospectivity of Nigeria's inland basins from the viewpoint of organic geochemistry and organic petrology. *American Association of Petroleum Geologists Bulletin*, 88, 325 – 353
- Obaje, N.G., Moumouni, A., Goki, N.G. and Chaanda, M.S. 2011. Stratigraphy, paleogeography and Hydrocarbon resource potentials of the Bida Basin in North- Central Nigeria. *Journal of Mining and Geology* v.47(2), p.97-114
- Ojo SB, Ajakaiye DE (1976) Preliminary interpretation of gravity measurements in the Mid-Niger Basin area, Nigeria. In: Kogbe CA (ed) *Geology of Nigeria*, 2nd edn, Elizabethan Publishers, Lagos, pp 347-358.
- Ojo, O. J and Akande, S. O. 2009. Sedimentology and depositional environments of the Maastrichtian Patti Formation, southern Bida Basin, Nigeria. *Cretaceous Research*, 30, 1415-1425.
- Ojo, O.J. and Akande, S.O. 2003. Facies relationships and depositional environments of the Upper Cretaceous Lokoja Formation in the Bida Basin, Nigeria. *Journal of Mining and Geology* 39, 39-48.
- Ojo, O.J. and Akande, S.O. 2006. Sedimentological and palynological studies of the Patti Formation, southern Bida basin, Nigeria: implications for paleoenvironments and paleogeography: *Nigerian Association of Petroleum Explorationists Bulletin* 19: 61-77
- Okunlola, O.A. and Idowu, O. 2012. The geochemistry of claystone-shale deposits from the Maastrichtian Patti Formation, Southern Bida basin, Nigeria. *Earth Sci. Res. SJ*. 16 (2): 57- 67
- Petters SW (1978) Middle Cretaceous paleoenvironments and biostratigraphy of the Benue Trough, Nigeria. *Geol Soc Am Bull* 89:151-154

- Pettijohn, F. J. (1963). *Chemical composition of sandstones, excluding carbonate and volcanic sands: Representative analyses* (Vol. 440). US Govt. Print. Off.
- Pettijohn, F. J. (1987). *Sand and sandstone*. Springer. <http://dx.doi.org/10.1007/978-1-4612-1066-5>.
- Pettijohn, F.J., 1975. *Sedimentary rocks*. Harper and Row, New York (3<sup>rd</sup> Ed.), 628p.
- Reyment, R.A., 1965. *Aspects of the Geology of Nigeria: The Stratigraphy of the Cretaceous and Cenozoic Deposits*. Ibadan University Press, p.145
- Roser B. P., Korsch R. J., 1986. Determination of tectonic setting of sandstone – mudstone suites using SiO<sub>2</sub> content and K<sub>2</sub>O/Na<sub>2</sub>O ratio, *J. Geol.* 94, 635 – 650.
- Roser, B.P. and Korsch, R.J. 1986. Determination of tectonic setting of sandstone mudstone suites using SiO content and KO/NaO ratio. *Jour. Geol.* 94, 635–650.
- Sam Boggs, Jr. (1987): *Principles of Sedimentology and Stratigraphy*, Macmillan Publishing Company New York pp. 105 -121.
- Sam Boggs, Jr. (2006)): *Principles of Sedimentology and Stratigraphy*, fourth edition, Pearson education Inc. Upper Saddle Rivers, USA. P. 581
- Sames, C.W., *Journal of Sedimentary Petrology*, 36, 1966, pp. 126-142.
- Sneed, E.D. and Folk, R.E. 1958. Pebbles in the lower Colorado River, Texas: a study of particlemorphogenesis. *Journal of Geology*, 66, pp. 114 – 150.
- Stratten, T. 1974. Notes on the application of shape parameters to differentiate between beach and riverdeposits in Southern Africa. *Trans. Geological Society of South Africa*, 77, pp. 59 – 64.
- Tijani, M.N., Nton, M.E. and Kitagawa, R. 2010. Textural and geochemical characteristics of the Ajali Sandstone, Anambra Basin, SE Nigeria: Implication for its provenance. *Comptes Rendus Geoscience*, 342, 136 – 150p.
- Wentworth, 1992. Grain size classification.
- Whiteman, A.J., 1982. *Nigeria: It's Petroleum Geology, resources and potential*. Vol.I and II. Graham and Trotham, London, 394 p.